Effects of Vapor–Liquid Mass Transfer on Feasibility of Reactive Distillation

Alberto Nisoli, Michael F. Doherty, and Michael F. Malone
Dept. of Chemical Engineering, University of Massachusetts, Amherst, MA 01003

DOI 10.1002/aic.10139
Published online in Wiley InterScience (www.interscience.wiley.com).

A cascade model including the Stefan–Maxwell model for mass transfer is developed to assess the feasibility of reactive distillation. The model fixed points are determined as a function of the Peclet number and other parameters, using a pseudo arc-length continuation method. The approach is illustrated with two examples: a parametric study of an idealized ternary system, and the esterification of acetic acid to produce isopropyl acetate. In the limit of little or no reaction, the fixed points are independent of the mass-transfer resistance, and a model based on phase equilibrium can be used for feasibility. When the chemical reaction rates or extents are more significant, the fixed points do depend on the Peclet number, and mass transfer can influence the feasible products. However, best estimates of the mass-transfer parameters and the processing conditions typical of reactive distillation indicate that these effects are small for the examples studied. © 2004 American Institute of Chemical Engineers *AIChE J,* 50: 1795–1813, 2004
Keywords: reactive distillation, vapor–liquid mass transfer, Stefan–Maxwell model, Peclet number, Damköhler number

Introduction and Background

Distillation accompanied by chemical reaction is a process alternative that has grown significantly in the last 15 years, according to the increasing number of articles and patents issued after 1990 (Malone and Doherty, 2000). Reactive distillation is potentially attractive because it often allows for the possibility of reducing capital and energy costs by simplifying the process. The most famous example of process simplification through the use of reactive distillation is the Eastman flow sheet for producing methyl acetate (Agreda and Partin, 1984; Agreda et al., 1990), and other applications offer similar benefits (Oyevaar et al., 2000).

The first step involved in the development of a reactive distillation process is the assessment of its feasibility. Feasibility methods have been developed extensively for simple distillation (Fidkowski et al., 1993; Wanschafft et al., 1992) and for reactive distillation with phase and chemical reaction equilibrium using reaction invariants (Barbosa and Doherty, 1988; Espinosa et al., 1995; Ung and Doherty, 1995a,b,c). Lately more work has been done on reactive distillation systems at finite reaction rates using a variety of approaches. In addition to optimization methods (Ciric and Gu, 1994; Ismail et al., 1999; Papalexandri and Pistikopoulos, 1996) three geometric methods have been developed: residue curve/bifurcation methods (Chadda et al., 2000; Rev, 1994; Thiel et al., 1997a,b; Venimadhavan et al., 1994, 1999); attainable region methods (Gadewar et al., 2002; McGregor et al., 1997; Nisoli et al., 1997); difference point methods (Lee et al., 2000a,b). Chadda et al. (2001) developed an algorithm for predicting feasible splits for continuous single–feed reactive distillation that is not limited by the number of reactions or components.

All of the approaches previously described assume that the liquid and vapor are at phase equilibrium, thus the vapor and liquid mole fractions are related by a K-value that can be calculated given pressure, temperature, composition and an appropriate thermodynamic model. To explain the deviation from phase equilibrium in real systems, multicomponent mass transfer has been described for both simple and reactive distillation using different models that are characterized by different

Correspondence concerning this article should be addressed to M. F. Malone at mmalone@ecs.umass.edu.

levels of complexity. The simplest model is a description of mass transfer using Murphree efficiencies in residue curve maps (Castillo and Towler, 1997, 1998) or in calculating minimum reflux ratio and minimum number of stages for distillation (Agarwal and Taylor, 1994). The development of more rigorous multicomponent mass-transfer models has grown significantly in the last ten years, corresponding to the increasing interest in reactive distillation especially for reactions involving esters and fuel ethers. Kooijman and Taylor (1995a) pointed out the advantage of modeling mass transfer in multicomponent distillation using the Stefan–Maxwell equations, showing that in some cases column designs based on phase equilibrium or efficiency methods can be less accurate than a high-fidelity mass-transfer model. They extended the model to dynamic simulation as well (Kooijman and Taylor, 1995b). Higler et al. (1998, 1999a,b, 2000) applied a Stefan–Maxwell mass-transfer model for simulating nonreactive and reactive distillation columns. In addition to emphasizing the importance of adopting a rigorous mass-transfer model vs. assuming phase equilibrium or a simplified efficiency model, they compared different flow regimes and mixing characteristics on a tray (mixed-flow model, single and multiple cell model with axial dispersion). Very detailed activity-based mass and heat transfer models for catalytic distillation of fuel ethers have been developed by Sundmacher and Hoffmann (1993, 1994). Thiel et al. (1997a,b) also used residue curve maps for fuel ether systems before formulating a rigorous mass-transfer model, although the residue curves were still calculated assuming phase equilibrium. Nonequilibrium residue curve maps were recently addressed by Sridhar et al. (2002). A comprehensive review of mass-transfer models used in reactive distillation was published by Taylor and Krishna (2000).

All of the mass-transfer models for reactive and catalytic distillation mentioned above were targeted to accurately simulate the performance of columns, rather than addressing the feasibility of reactive distillation including mass-transfer effects. The focus of this article is on assessing the importance of mass transfer in conceptual design for determining feasibility of a reactive distillation process. We use the Stefan–Maxwell approach for mass transfer combined with the flash cascade model developed by Chadda et al. (2001). The main question relevant to feasibility is whether the topology and/or the location of the fixed points (that is, product feasibility) in the composition space change as a result of mass-transfer limitations.

The Flash Cascade Model

In a distillation column, each section (rectifying or stripping) can be represented by a countercurrent cascade of flashes. For the purpose of estimating feasible product compositions we can greatly simplify the cascade by removing the countercurrent recycles of liquid and vapor flows between successive flash units as shown in Figure 1. It has been observed that transforming a countercurrent flash cascade into a cocurrent cascade only affects the *recovery* of the key components without significantly changing the product composition, which is the focus of a feasibility analysis (Chadda et al., 2001; Doherty and Malone, 2001; Henley and Seader, 1981, sec. 7.6). Therefore the simpler cocurrent model can be used to assess feasibility of reactive distillation in continuous columns.

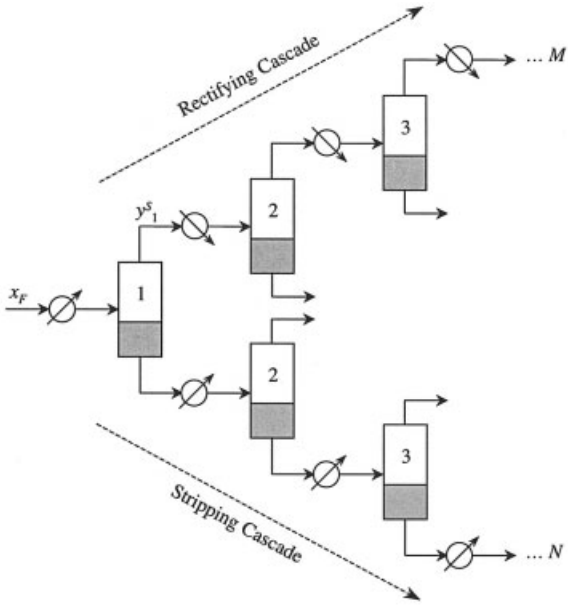

Figure 1. Rectifying and stripping flash cascades (Chadda et al., 2001).

Each flash device in Figure 1 is a two-phase continuously stirred tank reactor (CSTR). We make the following assumptions:

- Chemical reaction occurs only in the liquid phase.
- Steady-state conditions.
- Each device in the cascade operates at the same constant pressure, whereas the temperature changes according to the boiling point of the mixture (P, ϕ flash).
- Mole fractions and activity-based kinetic models are used for the reasons explained in Venimadhavan et al. (1994) and Nisoli et al. (1997).

For the general case of nonequimolar chemical reaction [where we define the dimensionless parameters in terms of mass instead of moles (Nisoli et al., 1997)] the system of algebraic equations describing the stripping cascade can be written as

$$(x_{i,j} - x_{i,j-1}) = \phi_m \frac{M(\mathbf{x}_{j-1})}{M(\mathbf{y}_j)}(x_{i,j} - y_{i,j}) + (\nu_i - \nu_T x_{i,j})\left(\frac{k_f}{k_{f,ref}}\right)\left(\frac{D}{1-D}\right)\frac{M(\mathbf{x}_{j-1})}{M(\mathbf{x}_j)} r(\mathbf{x}_j) \quad i = 1, \ldots, C-1 \qquad j = 1, 2, \ldots, N \quad (1)$$

where $x_{i,j}$ and $y_{i,j}$ are the mole fractions of component i in the jth device of the cascade in the liquid phase and the vapor phase, respectively. The initial condition of the difference equation is $\mathbf{x}_0 = \mathbf{x}_F$. The corresponding model for the rectifying cascade is

$$(x_{i,j} - y_{i,j-1}) = \phi_m \frac{M(\mathbf{y}_{j-1})}{M(\mathbf{y}_j)}(x_{i,j} - y_{i,j}) + (\nu_i - \nu_T x_{i,j})\left(\frac{k_f}{k_{f,ref}}\right)\left(\frac{D}{1-D}\right)\frac{M(\mathbf{y}_{j-1})}{M(\mathbf{x}_j)} r(\mathbf{x}_j) \quad i = 1, \ldots, C-1 \qquad j = 2, 3, \ldots, M \quad (2)$$

that has $\mathbf{y}_1 = \mathbf{y}_1^s$ as the initial condition. The model is formulated in terms of two dimensionless parameters: ϕ_m is the mass fraction of feed vaporized in each unit and Da is the Damköhler number (Damköhler, 1939; Venimadhavan et al., 1999), which has been scaled in the parameter D to vary from 0 (no reaction) to unity (reaction equilibrium)

$$D = \left(\frac{\text{Da}}{1 + \text{Da}}\right) \tag{3}$$

The dimensionless quantities, D and ϕ_m in these equations, are defined with respect to mass flows and mass holdups $\{D = \text{Da}/(1 + \text{Da})$, $\text{Da} = [(H_{m,j}/L_{m,j-1})/(1/k_{f,ref})]$, and $\phi_m = V_{m,j}/L_{m,j-1}$ (stripping cascade), or $\text{Da} = [(H_{m,j}/V_{m,j-1})/(1/k_{f,ref})]$, and $\phi_m = V_{m,j}/V_{m,j-1}$ (rectifying cascade)$\}$. $M(\mathbf{x})$ and $M(\mathbf{y})$ are the average molecular weights for the liquid and vapor phases, respectively.

For a given feed composition, these cascades are solved recursively for N, $M \rightarrow \infty$. When there is no change in successive iterates, a stable fixed point has been reached. The fixed points are the fundamental limits to the trajectories, and thus represent the feasible product compositions, just as the singular points in residue curve maps determine feasible products in nonreactive distillation. Therefore, the fixed points $\hat{\mathbf{x}}$ for the stripping cascade are solutions of

$$(1 - D)\frac{M(\hat{\mathbf{x}})}{M(\hat{\mathbf{y}})}(\hat{x}_i - \hat{y}_i) + (\nu_i - \nu_T\hat{x}_i)\left(\frac{k_f}{k_{f,ref}}\right)\left(\frac{D}{\phi_m}\right)r(\hat{\mathbf{x}}) = 0 \qquad i = 1, \ldots, C - 1 \tag{4}$$

Similarly, the fixed points, $\hat{y}$, for the rectifying cascade are solutions of

$$(1 - D)\frac{M(\hat{\mathbf{x}})}{M(\hat{\mathbf{y}})}(\hat{x}_i - \hat{y}_i) - (\nu_i - \nu_T\hat{x}_i)\left(\frac{k_f}{k_{f,ref}}\right)\left(\frac{D}{1 - \phi_m}\right)r(\hat{\mathbf{x}}) = 0 \qquad i = 1, \ldots, C - 1 \tag{5}$$

where the sign has been changed (Chadda et al., 2001), for analogy between this work and the earlier work done in equilibrium reactive distillation (the stability of Eq. 5 is reversed; thus a stable fixed point obtained by solving recursively Eq. 2 for $M \rightarrow \infty$ corresponds to an unstable node in Eq. 5).

In the limit of no reaction ($D = 0$) and equilibrium chemical reaction ($D = 1$), the fixed-point criteria for both the stripping and rectifying cascades (Eqs. 4 and 5) reduce to the same equation. However, for $0 < D < 1$ (kinetically controlled regime) there are different fixed points for the stripping and rectifying cascades, which cannot be provided simultaneously by a simple distillation experiment (Chadda et al., 2001). Although the fixed points of a simple distillation experiment (Chiplunkar et al., 2001; Venimadhavan et al., 1999) are equivalent to the stripping cascade fixed points (potential bottoms from a continuous column), the potential distillates from a continuous column can be estimated only by solving Eq. 5. That is the key result of Chadda's feasibility study, which we use to analyze the effects of mass-transfer limitations on the fixed points of the flash cascades.

A useful tool for representing the fixed-point branches of interest is the *feasibility diagram*. Using a bifurcation analysis of the solutions $\hat{\mathbf{x}}(D)$ for Eqs. 4 and 5 we track the fixed-point branches of the flash cascade model for $0 \leq D < 1$ at $\phi = 0.5$. The branches of fixed points are calculated using the pseudo arc-length continuation method in AUTO (Doedel, 1986) and the boiling point of the mixture $T[\hat{\mathbf{x}}(D)]$ is used to represent the solution. The feasibility diagram shows only the unstable nodes in the rectifying bifurcation diagram (potential distillates from a continuous column) and the stable nodes in the stripping cascade (potential bottoms from a continuous column).

Mass-Transfer Model

In the cascade model of Chadda et al. (2001) the fixed points are calculated at vapor–liquid equilibrium between $\hat{y}$ and $\hat{x}$. In contrast we consider mass transfer. The liquid and vapor phases are distinguished into a bulk and a film, each characterized by a set of mole fractions (x and y for the bulk, x^I and y^I for the film interface). Liquid and vapor films are connected through the vapor–liquid interface at which phase equilibrium is assumed, that is, a "two-film theory" where x^I and y^I are at phase equilibrium. In our model we consider heat transfer to be very fast compared to mass transfer, so that the temperature in the liquid phase, in the vapor phase, and at the interface are all equal. We also assume that the liquid-phase chemical reaction in the liquid film is not significant (negligible liquid holdup in the interface). This assumption is valid unless the chemical reaction is very fast, which is generally not the case for reactive distillation. Taylor and Krishna (2000) developed a more general model, which accounts for chemical reaction in the liquid film. They also say that "for most reactive distillation the change in the fluxes through the film will not be significant because the Hatta numbers are smaller than unity" (Froment and Bishoff, 1990, p. 260; Sundmacher et al., 1994; Vas Bath et al., 1999a,b).

Each device in the stripping cascade is represented by the two-phase CSTR in Figure 2a. $N_{i,j}$ represents the interfacial mass-transfer rates, which are the product of molar flux and interfacial area. The arrow between liquid and vapor phases in Figure 2 indicates the sign convention for the positive direction of the flux. There are four sets of mass balances to represent each stage j of the cascade:

(1) Overall component and total mass balances:

$$L_{j-1}x_{i,j-1} - L_jx_{i,j} - V_jy_{i,j} + \nu_ik_fr(\mathbf{x}_j)H_j^L = 0 \qquad i = 1, \ldots, C - 1 \tag{6}$$

$$L_{j-1} - L_j - V_j + \nu_Tk_fr(\mathbf{x}_j)H_j^L = 0 \tag{7}$$

(2) Liquid-phase component and total mass balances:

$$L_{j-1}x_{i,j-1} - L_jx_{i,j} - N_{i,j}^L + \nu_ik_fr(\mathbf{x}_j)H_j^L = 0 \qquad i = 1, \ldots, C - 1 \tag{8}$$

$$L_{j-1} - L_j - \sum_{i=1}^{C} N_{i,j}^L + \nu_Tk_fr(\mathbf{x}_j)H_j^L = 0 \tag{9}$$

(3) Vapor-phase component and total mass balances:

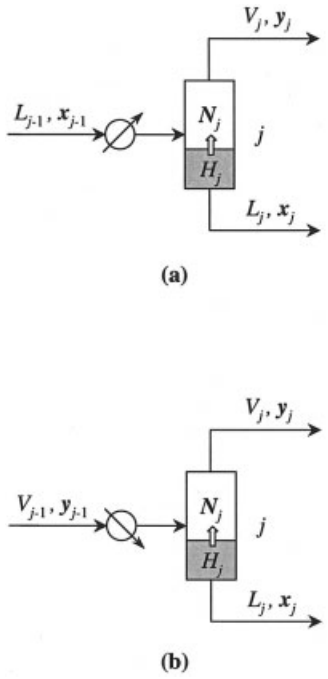

Figure 2. Two-phase flash with mass transfer for (a) stripping and (b) rectifying cascades.

$$N_{i,j}^V - V_j y_{i,j} = 0 \qquad i = 1, \ldots, C-1 \tag{10}$$

$$\sum_{i=1}^{C} N_{i,j}^V - V_j = 0 \tag{11}$$

(4) Interface mass balances:

$$N_{i,j}^L - N_{i,j}^V = 0 \qquad i = 1, \ldots, C \tag{12}$$

The first three sets of mass balances are not all independent. Any combination of two together with the interface mass balances (Eq. 12) can be used to model the system. In our derivation the liquid-phase mass balances and the overall mass balances will be coupled with the interface mass balances. In Eqs. 6, 8, and 10 the component index i goes from 1 to $C-1$ as the stoichiometry constraints are implicitly assumed ($\Sigma_{i=1}^{C} x_{i,j} = \Sigma_{i=1}^{C} y_{i,j} = 1$). Equations 6 and 7 (corresponding to Eqs. 2 and 1, respectively, in Chadda et al., 2001) can be rearranged and put in dimensionless form to give the stripping cascade (Eq. 1).

In addition to the mass balances we introduce two sets of constitutive equations to define the liquid and vapor mass-transfer rates in terms of the sum of a diffusive contribution and a convective contribution. For the liquid phase we have

$$N_{i,j}^L = \rho_j^L \sum_{k=1}^{C-1} k_{i,k,j}^L (x_{k,j} - x_{k,j}^I) A_j + x_{i,j} N_{T,j}^L \qquad i = 1, \ldots, C-1 \tag{13}$$

where ρ_j^L is the molar density in the liquid phase ($\rho_j^L = H_j^L / v_j^L$, where v_j^L is the total liquid volume); $k_{i,k,j}^L$ represents the matrix elements [$(C-1) \times (C-1)$] of liquid-phase multicomponent mass-transfer coefficients; $x_{k,j}^I$ represents the liquid mole fractions at the interface for the jth stage of the stripping cascade; A_j is the interfacial area; and $N_{T,j}^L$ is the sum of the mass-transfer rates ($N_{T,j}^L = \Sigma_{i=1}^{C} N_{i,j}^L$). The mass-transfer rates for the vapor phase are defined as

$$N_{i,j}^V = \rho_j^V \sum_{k=1}^{C-1} k_{i,k,j}^V (y_{k,j}^I - y_{k,j}) A_j + y_{i,j} N_{T,j}^V \qquad i = 1, \ldots, C-1 \tag{14}$$

where ρ_j^V is the molar density in the vapor phase ($\rho_j^V = H_j^V / v_j^V$, where v_j^V is the total vapor volume), $k_{i,k,j}^V$ represents the matrix elements [$(C-1) \times (C-1)$] of vapor-phase multicomponent mass-transfer coefficients, and $y_{k,j}^I$ are the vapor mole fractions at the interface for the jth stage of the stripping cascade.

Phase equilibrium is assumed at the vapor–liquid interface, where the component mole fractions are related by a vapor–liquid equilibrium (VLE) relation

$$y_{i,j}^I = K_{i,j}^I x_{i,j}^I \qquad i = 1, \ldots, C \tag{15}$$

By combining the $4C-2$ (Eqs. 8, 9, 12, 13, and 14) we can eliminate the $2C$ mass-transfer rates and obtain the following $2C-2$ relationships

$$\rho_j^L \sum_{k=1}^{C-1} k_{i,k,j}^L (x_{k,j} - x_{k,j}^I) A_j + L_{j-1}(x_{i,j} - x_{i,j-1}) - (\nu_i - \nu_T x_{i,j}) k_f r(\mathbf{x}_j) H_j^L = 0) \qquad i = 1, \ldots, C-1 \tag{16}$$

$$\rho_j^V \sum_{k=1}^{C-1} k_{i,k,j}^V (y_{k,j}^I - y_{k,j}) A_j + L_j(x_{i,j} - y_{i,j}) - L_{j-1}(x_{i,j-1} - y_{i,j}) - (\nu_i - \nu_T y_{i,j}) k_f r(\mathbf{x}_j) H_j^L = 0 \qquad i = 1, \ldots, C-1 \tag{17}$$

Given the definition of total molar density ($\rho_j = H_j / v_j$) and interfacial area per unit volume ($a_j = A_j / v_j$), Eqs. 16 and 17 are equivalent to

$$\frac{H_j^L}{L_{j-1}} \sum_{k=1}^{C-1} k_{i,k,j}^L a_j^L (x_{k,j} - x_{k,j}^I) + (x_{i,j} - x_{i,j-1}) - (\nu_i - \nu_T x_{i,j}) \times \frac{k_f}{k_{f,ref}} r(\mathbf{x}_j) \frac{k_{f,ref} H_j^L}{L_{j-1}} = 0 \qquad i = 1, \ldots, C-1 \tag{18}$$

$$\frac{H_j^V}{L_{j-1}} \sum_{k=1}^{C-1} k_{i,k,j}^V a_j^V (y_{k,j}^I - y_{k,j}) + \frac{L_j}{L_{j-1}} (x_{i,j} - y_{i,j}) - (x_{i,j-1} - y_{i,j}) - (\nu_i - \nu_T y_{i,j}) \frac{k_f}{k_{f,ref}} r(\mathbf{x}_j) \frac{k_{f,ref} H_j^L}{L_{j-1}} = 0 \qquad i = 1, \ldots, C-1 \tag{19}$$

We can introduce the same dimensionless parameters (Da and ϕ_m) used for the equilibrium cascade model, expressed in mass quantities

$$\frac{k_{f,ref}H_j^L}{L_{j-1}} = \mathrm{Da}\,\frac{M(\mathbf{x}_{j-1})}{M(\mathbf{x}_j)} \tag{20}$$

$$\frac{L_j}{L_{j-1}} = (1-\phi_m)\,\frac{M(\mathbf{x}_{j-1})}{M(\mathbf{x}_j)} \tag{21}$$

We also introduce reference mass-transfer coefficients k_{ref}^L and k_{ref}^V for the liquid and vapor phase, respectively, for the purpose of setting up the model in dimensionless form. The group $H_j^L k_{ref}^L a_j^L/L_{j-1}$ represents a characteristic residence time (H_j^L/L_{j-1}) divided by a characteristic mass-transfer time [$1/(k_{ref}^L a_j^L)$], which is equivalent to the inverse of a Peclet number:

$$\frac{\text{residence time}}{\text{mass transfer time}} = \frac{H_j^L/L_{j-1}}{1/(k_{ref}^L a_j^L)} = \frac{1}{\mathrm{Pe}_j^L} \tag{22}$$

We can also define a Pe number for the vapor phase

$$\frac{H_j^V k_{ref}^V a_j^V}{L_{j-1}} = \frac{1}{\mathrm{Pe}_j^V} \tag{23}$$

Because the model already assumes that Da and ϕ_m do not change from stage to stage, we make a similar assumption for Pe_j

$$\mathrm{Pe}_1^L = \mathrm{Pe}_2^L = \cdots = \mathrm{Pe}_j^L = \cdots = \mathrm{Pe}_N^L = \mathrm{Pe}^L \tag{24}$$

$$\mathrm{Pe}_1^V = \mathrm{Pe}_2^V = \cdots = \mathrm{Pe}_j^V = \cdots = \mathrm{Pe}_N^V = \mathrm{Pe}^V \tag{25}$$

Also for the general case of nonequimolar chemical reaction it is more convenient to define the dimensionless parameters in terms of mass quantities instead of molar quantities. Using mass quantities, Pe_j can be expressed as

$$\mathrm{Pe}_j^L = \frac{L_{j-1}}{H_j^L k_{ref}^L a_j^L} = \frac{L_{m,j-1}}{H_{m,j}^L k_{ref}^L a_j^L}\frac{M(\mathbf{x}_j)}{M(\mathbf{x}_{j-1})} = \mathrm{Pe}_{m,j}^L\frac{M(\mathbf{x}_j)}{M(\mathbf{x}_{j-1})} \tag{26}$$

$$\mathrm{Pe}_j^V = \frac{L_{j-1}}{H_j^V k_{ref}^V a_j^V} = \frac{L_{m,j-1}}{H_{m,j}^V k_{ref}^V a_j^V}\frac{M(\mathbf{y}_j)}{M(\mathbf{x}_{j-1})} = \mathrm{Pe}_{m,j}^V\frac{M(\mathbf{y}_j)}{M(\mathbf{x}_{j-1})} \tag{27}$$

Note that once the values of $k_{f,ref}$ and $k_{ref}a$ are specified, Da and Pe are not independent [Da $\times$ Pe $= k_{f,ref}/(k_{ref}a)$]. In a real system for which the holdup and flow rate (and therefore the residence time) have been specified, fixing a value of Pe is equivalent to setting an interfacial area. If we substitute the dimensionless parameters Da, ϕ_m, and the Peclet numbers into Eqs. 18 and 19 we obtain

$$\frac{1}{\mathrm{Pe}_m^L}\frac{M(\mathbf{x}_{j-1})}{M(\mathbf{x}_j)}\sum_{k=1}^{C-1}\frac{k_{i,k,j}^L}{k_{ref}^L}(x_{k,j}-x_{k,j}^I) + (x_{i,j}-x_{i,j-1}) - \mathrm{Da}\,\frac{M(\mathbf{x}_{j-1})}{M(\mathbf{x}_j)}(\nu_i-\nu_T x_{i,j})\frac{k_f}{k_{f,ref}}r(\mathbf{x}_j) = 0 \qquad i = 1,\ldots,C-1 \tag{28}$$

$$\frac{1}{\mathrm{Pe}_m^V}\frac{M(\mathbf{x}_{j-1})}{M(\mathbf{y}_j)}\sum_{k=1}^{C-1}\frac{k_{i,k,j}^V}{k_{ref}^V}(y_{k,j}^I-y_{k,j}) + (1-\phi_m)\frac{M(\mathbf{x}_{j-1})}{M(\mathbf{x}_j)}\times(x_{i,j}-y_{i,j}) - (x_{i,j-1}-y_{i,j}) - \mathrm{Da}\,\frac{M(\mathbf{x}_{j-1})}{M(\mathbf{x}_j)}\times(\nu_i-\nu_T y_{i,j})\frac{k_f}{k_{f,ref}}r(\mathbf{x}_j) = 0 \qquad i = 1,\ldots,C-1 \tag{29}$$

Equations 28 and 29, together with a VLE model relating $y_{i,j}^I$ to $x_{i,j}^I$ are solved together with the stripping cascade (Eq. 1). The model has four parameters, Da, ϕ, Pe^L, and Pe^V, which are either mass-based or molar-based quantities depending on the chemistry (nonequimolar or equimolar). By specifying a value of ϕ and assuming fast heat transfer, we eliminate the need for including the energy balances in the global system of equations. The model is solved for $x_{i,j}$, $x_{i,j}^I$, $y_{i,j}^I$, and $y_{i,j}$.

The fixed points of the cascade are given by solutions of the fixed-point equations

$$\frac{1}{\mathrm{Pe}_m^L}\sum_{k=1}^{C-1}\frac{k_{i,k}^L}{k_{ref}^L}(\hat{x}_k-\hat{x}_k^I) - \mathrm{Da}(\nu_i-\nu_T\hat{x}_i)\frac{k_f}{k_{f,ref}}r(\hat{\mathbf{x}}) = 0 \qquad i = 1,\ldots,C-1 \tag{30}$$

$$\frac{1}{\mathrm{Pe}_m^V}\frac{M(\hat{\mathbf{x}})}{M(\hat{\mathbf{y}})}\sum_{k=1}^{C-1}\frac{k_{i,k}^V}{k_{ref}^V}(\hat{y}_k^I-\hat{y}_k) - \phi_m(\hat{x}_i-\hat{y}_i) - \mathrm{Da}(\nu_i-\nu_T\hat{y}_i)\frac{k_f}{k_{f,ref}}r(\hat{\mathbf{x}}) = 0 \qquad i = 1,\ldots,C-1 \tag{31}$$

together with Eq. 4 and a VLE model relating $\hat{x}_i^I$ to $\hat{y}_i^I$.

The matrix of multicomponent liquid mass-transfer coefficients $[k^L]$ [of size $(C-1)\times(C-1)$] is calculated from the binary mass-transfer coefficients $\kappa_{i,k}^L$ (elements of $C \times C$ symmetric matrix) according to the Stefan–Maxwell equations

$$[k^L] = [R^L]^{-1}[\Gamma] \tag{32}$$

where

$$R_{i,i}^L = \frac{x_i}{\kappa_{i,C}^L} + \sum_{k=1,k\neq i}^{C}\frac{x_k}{\kappa_{i,k}^L} \tag{33}$$

$$R_{i,k}^L = -x_i\left(\frac{1}{\kappa_{i,k}^L} - \frac{1}{\kappa_{i,C}^L}\right) \tag{34}$$

$[\Gamma]$ is the matrix of thermodynamic factors that account for the nonideality of the liquid phase (Taylor and Kooijman, 1991; Taylor and Krishna, 1993, p. 24)

$$\Gamma_{i,k} = \delta_{i,k} + x_i \left.\frac{\partial \ln \gamma_i}{\partial x_k}\right|_{T,P,l\neq k=1,2\cdots C-1} \tag{35}$$

Depending on the nonideality of the liquid mixture the correction attributed to the thermodynamic factors might be significant. The matrix $[k^L]$ is evaluated at the composition $\bar{x}_i$, which is the average of bulk and interface composition (Taylor and Krishna, 1993, p. 215)

$$\bar{x}_i = \frac{x_i + x_i^I}{2} \tag{36}$$

Similarly, the matrix of the multicomponent mass-transfer coefficients for the vapor phase (assumed to follow an ideal behavior) is obtained according to the following equations

$$[k^V] = [R^V]^{-1} \tag{37}$$

where

$$R^V_{i,i} = \frac{y_i}{\kappa^V_{i,C}} + \sum_{k=1,k\neq i}^{C} \frac{y_k}{\kappa^V_{i,k}} \tag{38}$$

$$R^V_{i,k} = -y_i\left(\frac{1}{\kappa^V_{i,k}} - \frac{1}{\kappa^V_{i,C}}\right) \tag{39}$$

$[k^V]$ is also evaluated at the average between bulk and interface compositions in the vapor phase.

The calculation sequence for determining the fixed points is the following:

(1) Specify physical properties of the system (molecular weights, VLE parameters, pressure P, binary mass-transfer coefficients $\kappa^L_{i,k}$, $\kappa^V_{i,k}$).
(2) Assign values to the parameters ϕ_m, D, Pe^L_m, and Pe^V_m.
(3) Provide initial guesses for $\hat{x}_i$, $\hat{x}^I_i$, and $\hat{y}_i$.
(4) Calculate $\hat{y}^I_i$ and T from VLE and $\hat{x}^I_i$.
(5) Calculate $[\Gamma]$, $[R^L]$, and $[R^V]$.
(6) Calculate $[k^L]$ and $[k^V]$.
(7) Solve simultaneously the mass-transfer and VLE equations (Eqs. 30 and 31), and the fixed-point cascade (Eq. 4) for $\hat{x}_i$, $\hat{x}^I_i$, and $\hat{y}_i$, updating the calculations in steps (4), (5), and (6) at each iteration.

It can be shown that the rectifying cascade equations (analogous to the stripping cascade Eqs. 28 and 29) for the jth stage (Figure 2b) are

$$\frac{1}{\mathrm{Pe}^L_m}\frac{M(\mathbf{y}_{j-1})}{M(\mathbf{x}_j)}\sum_{k=1}^{C-1}\frac{k^L_{i,k,j}}{k^L_{ref}}(x_{k,j} - x^I_{k,j}) - (\nu_i - \nu_T x_{i,j})\frac{M(\mathbf{y}_{j-1})}{M(\mathbf{x}_j)} \times Da\,\frac{k_f}{k_{f,ref}}\,r(\mathbf{x}_j) = 0 \qquad i = 1,\ldots,C-1 \tag{40}$$

$$\frac{1}{\mathrm{Pe}^V_m}\frac{M(\mathbf{y}_{j-1})}{M(\mathbf{y}_j)}\sum_{k=1}^{C-1}\frac{k^V_{i,k,j}}{k^V_{ref}}(y^I_{k,j} - y_{k,j}) + \frac{M(\mathbf{y}_{j-1})}{M(\mathbf{x}_j)} \times (1-\phi_m)(x_{i,j} - y_{i,j}) - (\nu_i - \nu_T y_{i,j}) \times \frac{M(\mathbf{y}_{j-1})}{M(\mathbf{x}_j)}\,\mathrm{Da}\,\frac{k_f}{k_{f,ref}}\,r(\mathbf{x}_j) = 0 \qquad i = 1,\ldots,C-1 \tag{41}$$

where $\mathrm{Pe}^L_m = V_{m,j-1}/(H^L_{m,j}k^L_{ref}a^L_j)$ and $\mathrm{Pe}^V_m = V_{m,j-1}/(H^V_{m,j}k^V_{ref}a^V_j)$. The corresponding fixed-point equations for the rectifying cascade are

$$\frac{1}{\mathrm{Pe}^L_m}\sum_{k=1}^{C-1}\frac{k^L_{i,k}}{k^L_{ref}}(\hat{x}_k - \hat{x}^I_k) - (\nu_i - \nu_T\hat{x}_i)\mathrm{Da}\,\frac{k_f}{k_{f,ref}}\,r(\hat{\mathbf{x}}) = 0 \qquad i = 1,\ldots,C-1 \tag{42}$$

$$\frac{1}{\mathrm{Pe}^V_m}\sum_{k=1}^{C-1}\frac{k^V_{i,k}}{k^V_{ref}}(\hat{y}^I_k - \hat{y}_k) + \frac{M(\hat{\mathbf{y}})}{M(\hat{\mathbf{x}})}(1-\phi_m)(\hat{x}_i - \hat{y}_i) - (\nu_i - \nu_T\hat{y}_i) \times \frac{M(\hat{\mathbf{y}})}{M(\hat{\mathbf{x}})}\,\mathrm{Da}\,\frac{k_f}{k_{f,ref}}\,r(\hat{\mathbf{x}}) = 0 \qquad i = 1,\ldots,C-1 \tag{43}$$

Equations 42, 43, and VLE are solved in conjunction with Eq. 5. The calculation sequence for determining the fixed points is the same as that for the stripping cascade, except that the equations are solved for $\hat{y}_i$ instead of $\hat{x}_i$.

It can be shown (see Appendix) that the fixed-point equations are independent of the vapor-phase mass transfer; that is, for any value of Pe^V the bulk vapor mole fractions coincide with the vapor interface mole fractions ($\hat{y}_i = \hat{y}^I_i$). This also holds true in the stripping section, for the stage-to-stage cascade calculation, in a situation similar to multicomponent condensation (Taylor and Krishna, 1993, Chapter 15), where in the absence of liquid-phase reaction the liquid bulk and interface mole fractions coincide ($\hat{x}_i = \hat{x}^I_i$).

When $\mathrm{Pe} \to 0$ we recover the phase equilibrium case. In fact, when $\mathrm{Pe} \to 0$ the characteristic mass-transfer time is very small compared to the residence time, which means that the mass-transfer coefficients are very high

$$\mathrm{Pe}^L_m = \frac{\text{mass transfer time}}{\text{residence time}} = \frac{1/(k^L_{ref}a^L)}{H^L_m/L_m} \ll 1 \Rightarrow k^L_{ref}a^L \gg 1 \tag{44}$$

If the mass-transfer coefficients are very high, the mass-transfer rates are also very fast; therefore the concentration gradients across the liquid and vapor films must be very small ($x_i \to x^I_i$ and $y_i \to y^I_i$) and the limit of phase equilibrium is reached.

Example 1: Constant Volatility Mixture

We will now repeat an example that has been worked out for the phase-equilibrium case, with the purpose of comparing the results when mass-transfer resistance is taken into account.

Consider the following equilibrium-limited chemical reaction:

Table 1. Antoine Constants for Example 1*

Component	a_i	b_i	c_i
A	23.9226	−4025.76	0
B	23.4138	−4025.76	0
C	22.3147	−4025.76	0

*The form of the Antoine equation is $\ln P_i^{sat} = a_i + b_i/(T + c_i)$ with P_i in Pa and T in K.

$$A + B \rightleftharpoons C \tag{45}$$

We choose an equilibrium constant $K_{eq} = 2$, independent of temperature. The rate of reaction per mole of liquid is given by the expression

$$r = k_f\left(x_A x_B - \frac{x_C}{K_{eq}}\right) \tag{46}$$

The molecular weights of A, B, and C are 86.2, 100.2, and 186.4, respectively. The normal boiling points are 51.6, 65.5, and 100°C, respectively, with constant relative volatilities $\alpha_{AC} = 5$, $\alpha_{BC} = 3$, and $\alpha_{CC} = 1$ (Doherty and Malone, 2001, p. 431). The Antoine constants used for calculating the boiling point of the pure components and the mixture are listed in Table 1. We assume $k_f/k_{f,ref} = 1$ (that is, forward rate constant independent of temperature) and $\phi_m = 0.5$ for all cases. Specifying a different value of ϕ, rather than 0.5, is just going to shift the fixed-point curves along the D-axis (for a fixed value of Pe specifying a different value of ϕ will change the value of D at which a bifurcation occurs). The fixed-point analysis of this ideal mixture has already been reported for the phase-equilibrium case (Doherty and Malone, 2001, p. 473; Venimadhavan et al., 1999). When we apply the fixed-point cascade model (Eqs. 4 and 5) to this specific example the following equations for the stripping and rectifying cascades, respectively, are solved

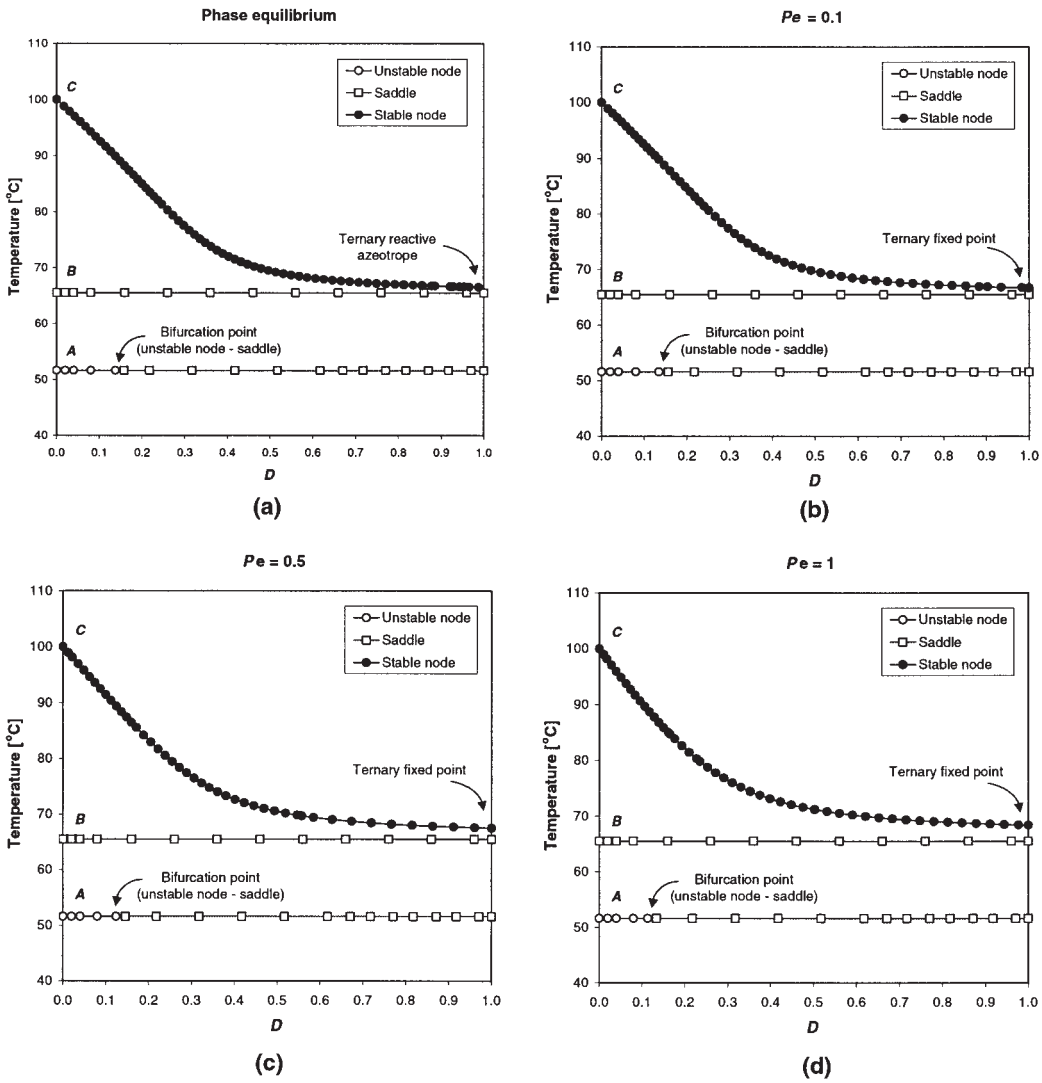

Figure 3. Stripping cascade bifurcation diagram (equal $\kappa_{i,k}$).

(a) Phase equilibrium case; (b) Pe = 0.1; (c) Pe = 0.5; (d) Pe = 1.

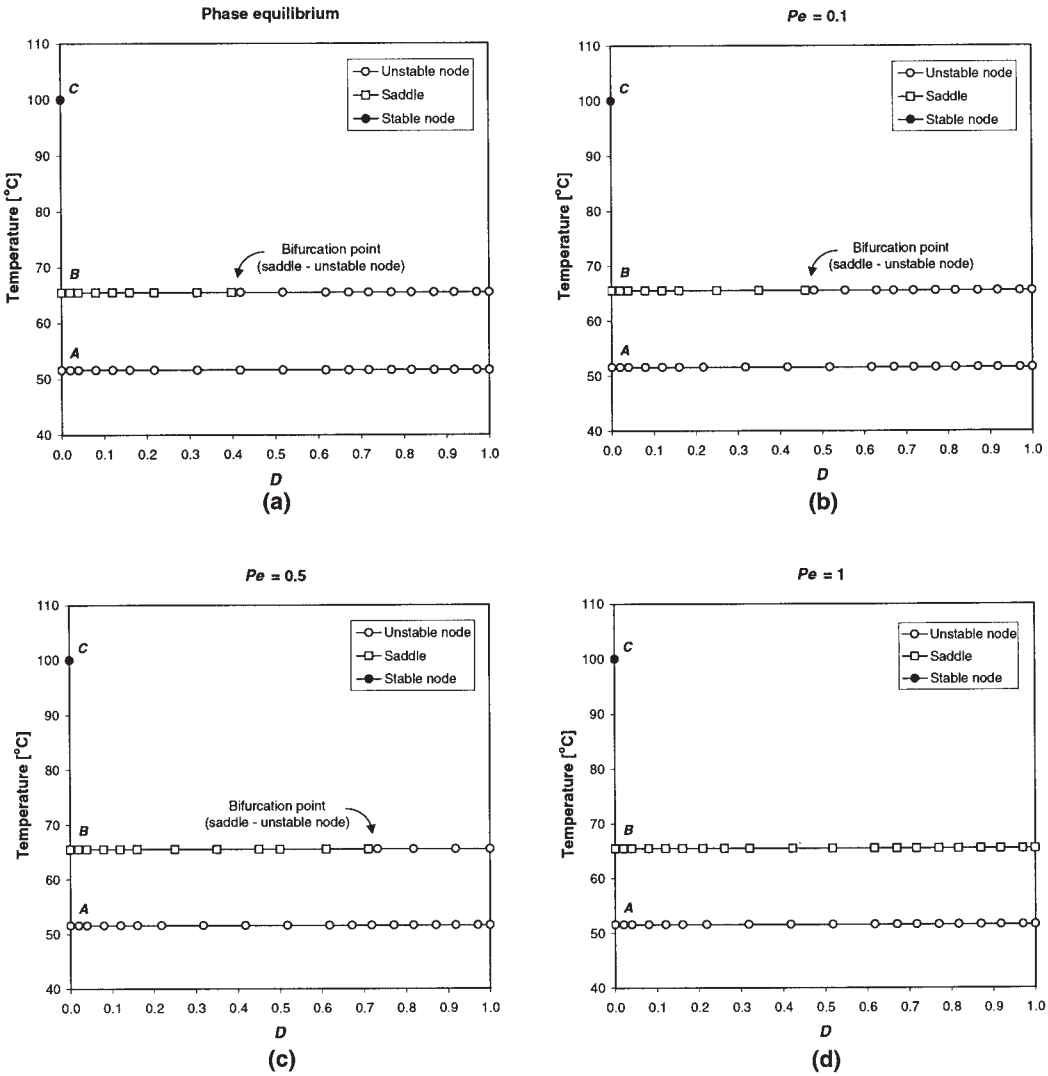

Figure 4. Rectifying cascade bifurcation diagram (equal $\kappa_{i,k}$).

(a) Phase equilibrium case; (b) Pe = 0.1; (c) Pe = 0.5; (d) Pe = 1.

$$(1 - D)\frac{M(\hat{\mathbf{x}})}{M(\hat{\mathbf{y}})}(\hat{x}_i - \hat{y}_i) + 2D\left(\hat{x}_1\hat{x}_2 - \frac{\hat{x}_3}{2}\right)(-1 + \hat{x}_i) = 0 \qquad i = 1, 2 \quad (47)$$

$$(1 - D)\frac{M(\hat{\mathbf{x}})}{M(\hat{\mathbf{y}})}(\hat{x}_i - \hat{y}_i) - 2D\left(\hat{x}_1\hat{x}_2 - \frac{\hat{x}_3}{2}\right)(-1 + \hat{x}_i) = 0 \qquad i = 1, 2 \quad (48)$$

The indices 1, 2, and 3 correspond to A, B, and C, respectively. Figure 3a shows the bifurcation diagram for the stripping cascade fixed points obtained in the absence of mass-transfer limitations. The corresponding bifurcation diagram for the rectifying fixed points is shown in Figure 4a. The unstable node branches of the rectifying cascade and the stable node branches of the stripping cascade are combined in the feasibility diagram shown in Figure 5a. Above $D \approx 0.4$, two unstable nodes are present, corresponding to the pure components A and B; either of the two is a possible distillate product, depending on the feed composition. The stable node branch is always a feasible bottoms product. Pure C is a feasible bottoms product only in the absence of reaction ($D = 0$); otherwise, the stable node contains all three components, so pure C is possible in the bottom only for a hybrid column with nonreactive stages below a reactive section.

In the present work we calculate the fixed points for the case of finite mass-transfer rates and compare them with those at phase equilibrium. We assume that the mass-transfer resistance occurs only in the liquid phase, given that we can show that Pe^V does not affect the fixed points (see Appendix); that is, $\mathrm{Pe}_m^V \to 0$ ($\hat{y}_i^I \to \hat{y}_i$). This eliminates Eqs. 31 and 43 from the model. For simplicity we refer to Pe_m^L as Pe in what follows. We first analyze the case of equal binary mass-transfer coefficients for all the components ($\kappa_{1,2} = \kappa_{1,3} = \kappa_{2,3} = \kappa$). In the case of an ideal mixture, the matrix of thermodynamic factors [Γ] reduces to the identity matrix, and the matrix of multicomponent mass-transfer coefficients (2×2) is simply given by

$$[k^L] = [R^L]^{-1} \quad (49)$$

where the elements of $[R^L]$ are given by Eqs. 33 and 34.

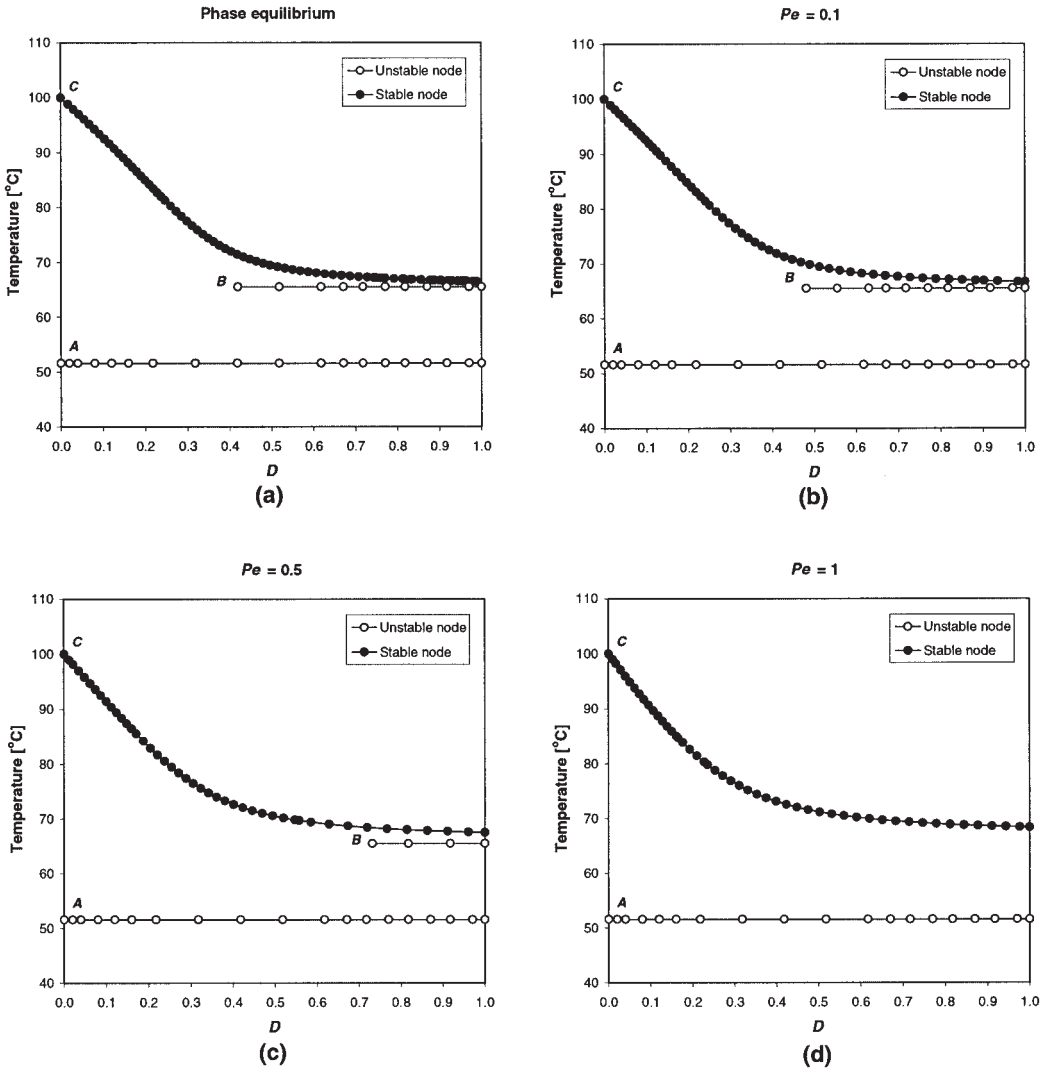

Figure 5. Feasibility diagram (equal $\kappa_{i,k}$).

(a) Phase equilibrium case; (b) Pe = 0.1; (c) Pe = 0.5; (d) Pe = 1.

When all of the $\kappa_{i,k}$ are the same then the matrix of multicomponent mass-transfer coefficients becomes

$$[k^L] = \begin{bmatrix} \kappa & 0 \\ 0 & \kappa \end{bmatrix} \tag{50}$$

which is independent of composition. In this specific case we choose $k^L_{ref} = \kappa$ and the mass-transfer Eq. 30 (for the stripping cascade) and Eq. 42 (for the rectifying cascade) reduce to

$$\frac{1}{\mathrm{Pe}}(\hat{x}_i - \hat{x}_i^I) - (-1 + \hat{x}_i)\mathrm{Da}\left(\hat{x}_1\hat{x}_2 - \frac{\hat{x}_3}{2}\right) = 0 \qquad i = 1, 2 \tag{51}$$

The fixed points of the stripping cascade are obtained by solving Eq. 51 together with Eq. 47 and the constant-volatility VLE model, which relates $\hat{y}_i^I$ to $\hat{x}_i^I$. Similarly, the fixed points of the rectifying cascade are obtained by solving Eq. 51 together with Eq. 48 and the constant-volatility VLE model. Beginning with a small value of Pe that approaches the limit of phase equilibrium, we increase Pe until significant changes in the bifurcation diagram are detected.

Figures 3b, c, and d show the bifurcation diagrams for the stripping cascade fixed points obtained for three different values of Pe. The corresponding bifurcation diagrams for the rectifying cascade fixed points are shown in Figures 4b, c, and d. The unstable node branches of the rectifying cascade and the stable node branches of the stripping cascade are combined in the feasibility diagrams (Figures 5b, 5c, and 5d).

In the limit of no reaction ($D \to 0$) the fixed points do not change regardless of the value of Pe. Therefore mass transfer does not affect feasibility for simple (nonreactive) distillation. The case of Pe = 0.1 (fast diffusion) is still close to the limit of phase equilibrium. As Pe increases, the ternary fixed point in the stripping cascade moves and the reactive azeotrope is no longer achieved as $D \to 1$, although the fixed points do lie on the reaction equilibrium curve in this limit (see Figure 6a). The bifurcation point in the pure A branch of the stripping cascade moves closer to the limit of no reaction ($D \to 0$) at higher Pe. The bifurcation point in the pure B branch of the rectifying

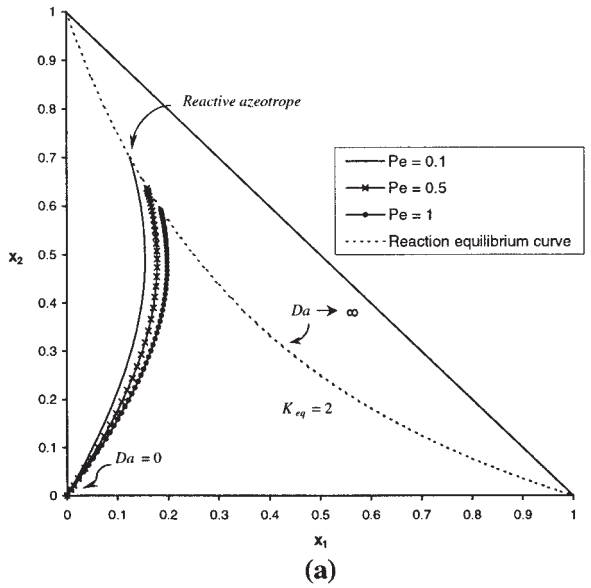

Figure 6. Pure C fixed-point branch vs. Da at different Pe.

(a) Stripping cascade (equal $\kappa_{i,k}$); (b) rectifying cascade (different $\kappa_{i,k}$).

cascade moves closer to the limit of reaction equilibrium ($D \rightarrow 1$) and eventually disappears for Pe = 1 (Figure 4d). Therefore, at Pe = 1 (Figure 5d) pure B is no longer a feasible distillate for any value of D.

Now consider a case where the binary mass-transfer coefficients for the different pairs are significantly different ($\kappa_{1,2} \neq \kappa_{1,3} \neq \kappa_{2,3}$). We choose $\kappa_{1,2} > \kappa_{1,3} > \kappa_{2,3}$ such that

$$\kappa_{1,2}/\kappa_{1,3} = 10$$

$$\kappa_{2,3}/\kappa_{1,3} = 0.5 \qquad (52)$$

For this case, the matrix of multicomponent mass-transfer coefficients is not constant, but is a function of composition. As a reference mass-transfer coefficient one can choose a multicomponent mass-transfer coefficient ($k_{i,k}$) or a binary mass-transfer coefficient ($\kappa_{i,k}$). Because the $k_{i,k}$ values depend on composition it is preferable to choose one of the binary mass-transfer coefficients. The highest off-diagonal term in the matrix of binary mass-transfer coefficients is a convenient choice for a ternary ideal mixture, given that for the entire range of composition $|k^L_{i,k}| \leq \max(\kappa_{i,k})$, so that the ratio $k^L_{i,k}/k^L_{ref}$ in Eqs. 30 and 42 is always between -1 and 1. The fixed points of the stripping cascade are obtained by solving Eq. 47 and the constant-volatility VLE model with the following mass-transfer equations (derived from Eq. 30)

$$\frac{1}{\mathrm{Pe}}\frac{1}{k_{ref}}[k^L_{i,1}(\hat{x}_1 - \hat{x}^I_1) + k^L_{i,2}(\hat{x}_2 - \hat{x}^I_2)] - (-1 + \hat{x}_i)\mathrm{Da}\left(\hat{x}_1\hat{x}_2 - \frac{\hat{x}_3}{2}\right) = 0 \qquad i = 1, 2 \quad (53)$$

Similarly, the fixed points of the rectifying cascade are calculated by solving Eq. 53 together with Eq. 48 and the constant-volatility VLE model. We report the fixed points of stripping and rectifying cascades for three different values of Pe: Pe = 0.1, Pe = 0.5, and Pe = 1; Pe $\approx$ 0.1 represents the maximum value of Pe for which the fixed points are still close to the limit of phase equilibrium. Then we keep increasing Pe until significant changes in the feasibility diagram are detected.

Figure 7 shows the bifurcation diagrams for the stripping cascade fixed points. The corresponding bifurcation diagrams for the rectifying cascade fixed points are shown in Figure 8. The unstable node branches of the rectifying cascade and the stable node branches of the stripping cascade are again combined in the feasibility diagrams (Figure 9). In Figures 8c and d the interruption in the branch of fixed points going from pure C to pure B is caused by some of the mole fraction values becoming negative (as in Figure 6b where the branch of fixed points moves outside the triangle before reaching pure B). Because compositions corresponding to negative mole fractions do not have physical meaning we did not report them in the bifurcation and feasibility diagrams. Pure B is a feasible distillate product only when the mass-transfer resistance is not very significant (low values of Pe), but as the mass-transfer resistance increases B becomes a possible bottom product for a large range of Damköhler numbers. As Pe increases, the mass-transfer resistances become more severe, and A tends to go to the vapor phase much more readily than either B or C. If enough reaction is present, C is depleted very quickly as the extent of the backward reaction is increased by the removal of A, and thus the liquid residue consists of pure B. These results for Pe = 1 are significantly different from those for the case of phase equilibrium. It should be noticed that such results were obtained assuming large differences in binary mass-transfer coefficients (up to a factor of 20; see Eq. 52). A very large difference in diffusivity (or binary mass-transfer coefficient) among binary pairs within the same mixture typically requires a substantial difference in viscosities [such as binary liquid diffusion coefficients at infinite dilution, like those calculated with the Wilke–Chang method (Reid et al., 1987, p. 598) that

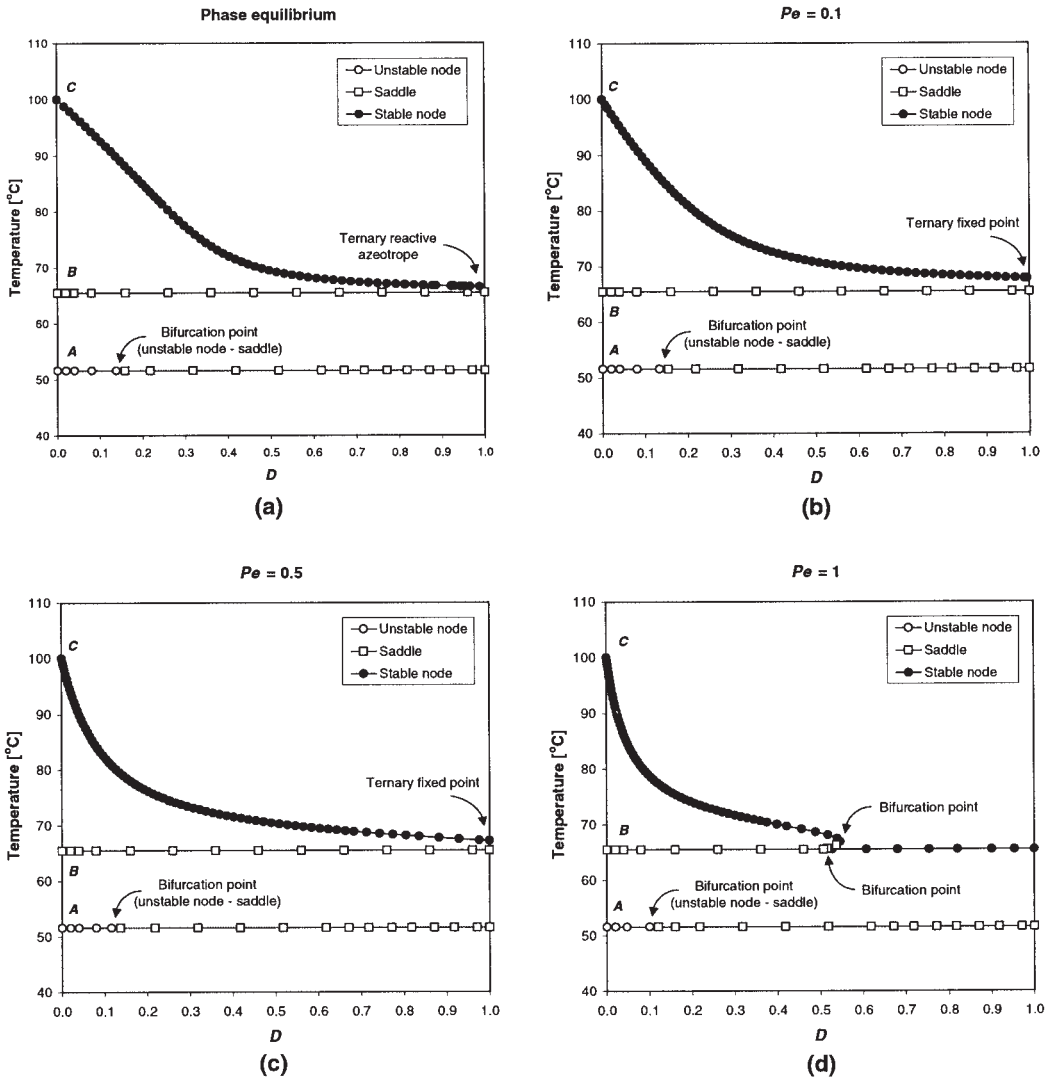

Figure 7. Stripping cascade bifurcation diagram (different $\kappa_{i,k}$).

(a) Phase equilibrium case; (b) Pe = 0.1; (c) Pe = 0.5; (d) Pe = 1.

we used in our next example, are inversely proportional to the viscosity of the solvent].

For comparison and verification of the results obtained with AUTO, we calculated the trajectories for two cases at low D, using an ordinary differential equation (ODE) model. The trajectories are calculated by solving a system of ODE's equivalent to the difference Eqs. 1 and 2. For the stripping cascade the following ODE system

$$\frac{dx_i}{d\xi} = \phi_m \frac{M(\mathbf{x})}{M(\mathbf{y})}(x_i - y_i) + (\nu_i - \nu_T x_i)\left(\frac{k_f}{k_{f,ref}}\right)\left(\frac{D}{1-D}\right) r(\mathbf{x}) \tag{54}$$

is solved in conjunction with the mass transfer Eq. 30. The stripping cascade with equal $\kappa_{i,k}$ at $D = 0.1$ and Pe $= 0.1$ exhibits a ternary fixed point (stable node) at $x_A = 0.035$ and $x_B = 0.068$, an unstable node at pure A, and a saddle at pure B (see Figure 3b). The phase plane for the stripping case is shown in Figure 10a, which is similar to the result obtained for phase equilibrium by Venimadhavan et al. (1999, Figure 2a). When the bifurcation occurs in the pure A branch at higher values of D, the unstable node moves away from pure A to a position outside the triangle, and A becomes a saddle (also see Venimadhavan et al., 1999; Figure 2b). The corresponding ODE system for the rectifying section (with the sign changed, according to Chadda et al., 2001) is

$$\frac{dy_i}{d\xi} = (1 - \phi_m)(x_i - y_i) - (\nu_i - \nu_T x_i) \times \left(\frac{k_f}{k_{f,ref}}\right)\frac{M(\mathbf{y})}{M(\mathbf{x})}\left(\frac{D}{1-D}\right) r(\mathbf{x}) \tag{55}$$

The system in Eq. 55 is solved together with the mass transfer Eq. 42. The rectifying cascade with $\kappa_{i,k}$, corresponding to Eq. 52 at $D = 0.1$ and Pe $= 0.5$, shows a stable node at $y_A = 0.062$ and $y_B = 0.317$, an unstable node at pure A, and a saddle at pure B (see Figure 8c). The resulting trajectories for the recti-

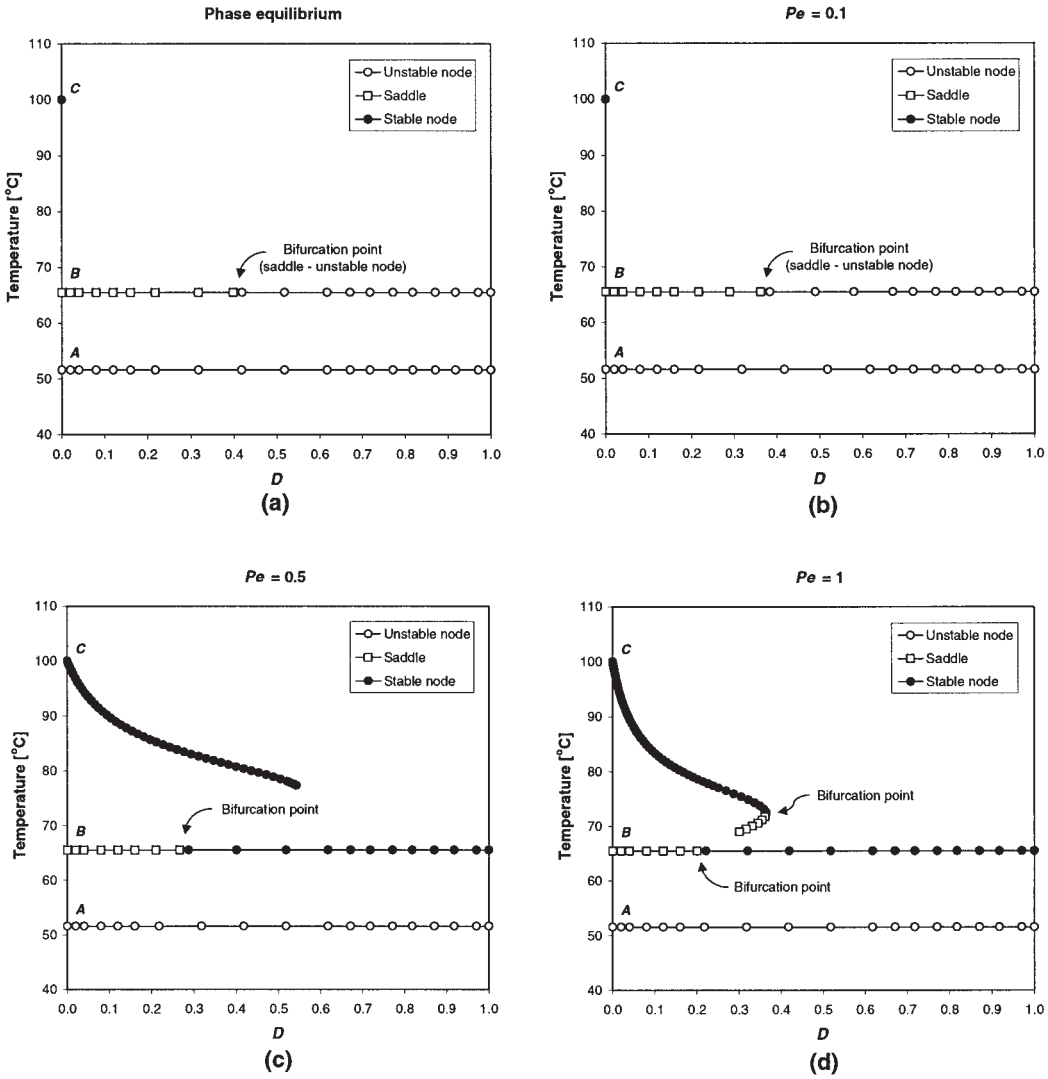

Figure 8. Rectifying cascade bifurcation diagram (different $\kappa_{i,k}$).

(a) Phase equilibrium case; (b) Pe = 0.1; (c) Pe = 0.5; (d) Pe = 1.

fying cascade are shown in Figure 10b. The phase planes reported in Figure 10 are completely consistent with the bifurcation diagrams in Figures 3b and 8c.

Example 2: Isopropyl Acetate

We want to apply this model to a real system that has already been studied for the case of phase equilibrium with the purpose of comparing the results of the fixed-point analysis when finite rates of mass transfer are included. For this purpose, we consider the esterification of acetic acid (HOAc) with isopropanol (IPA) at atmospheric pressure to produce isopropyl acetate (IPOAc) and water

$$\mathrm{HOAc} + \mathrm{IPA} \rightleftharpoons \mathrm{IPOAc} + \mathrm{H_2O} \tag{56}$$

We represent the kinetics using a pseudo-homogeneous model

$$r = k_f\left(a_1 a_2 - \frac{a_3 a_4}{K_{eq}}\right) \tag{57}$$

where the indices 1 to 4 correspond to HOAc, IPA, IPOAc, and water, respectively. The reaction equilibrium constant has a constant value of 8.7 in the temperature range of interest (Lee and Kuo, 1996), and we assume k_f to be independent of temperature [$(k_f/k_{f,ref}) = 1$]. This assumption was taken into account to allow comparison of the results with the previous work that was done on this system for the case of phase equilibrium (Chadda et al., 2001; Doherty and Malone, 2001, p. 474; Venimadhavan et al., 1999). Relaxing that assumption makes the value of the ratio $(k_f/k_{f,ref})$ vary between 1 and approximately 12.3 [given an apparent activation energy E_a of 16.4 kcal/mol, as reported by Manning (2000), and T_{ref} = 349.75 K (76.6°C, b.p. of the IPOAc–IPA–water ternary azeotrope)]. Calculations done using the ratio $(k_f/k_{f,ref})$ as a function of T have shown that the fixed-point analysis remains the same (same number of feasible branches with the same stability), the only difference being the position of the bifurcation points, which have slightly moved.

The thermodynamic model and physical property parameters

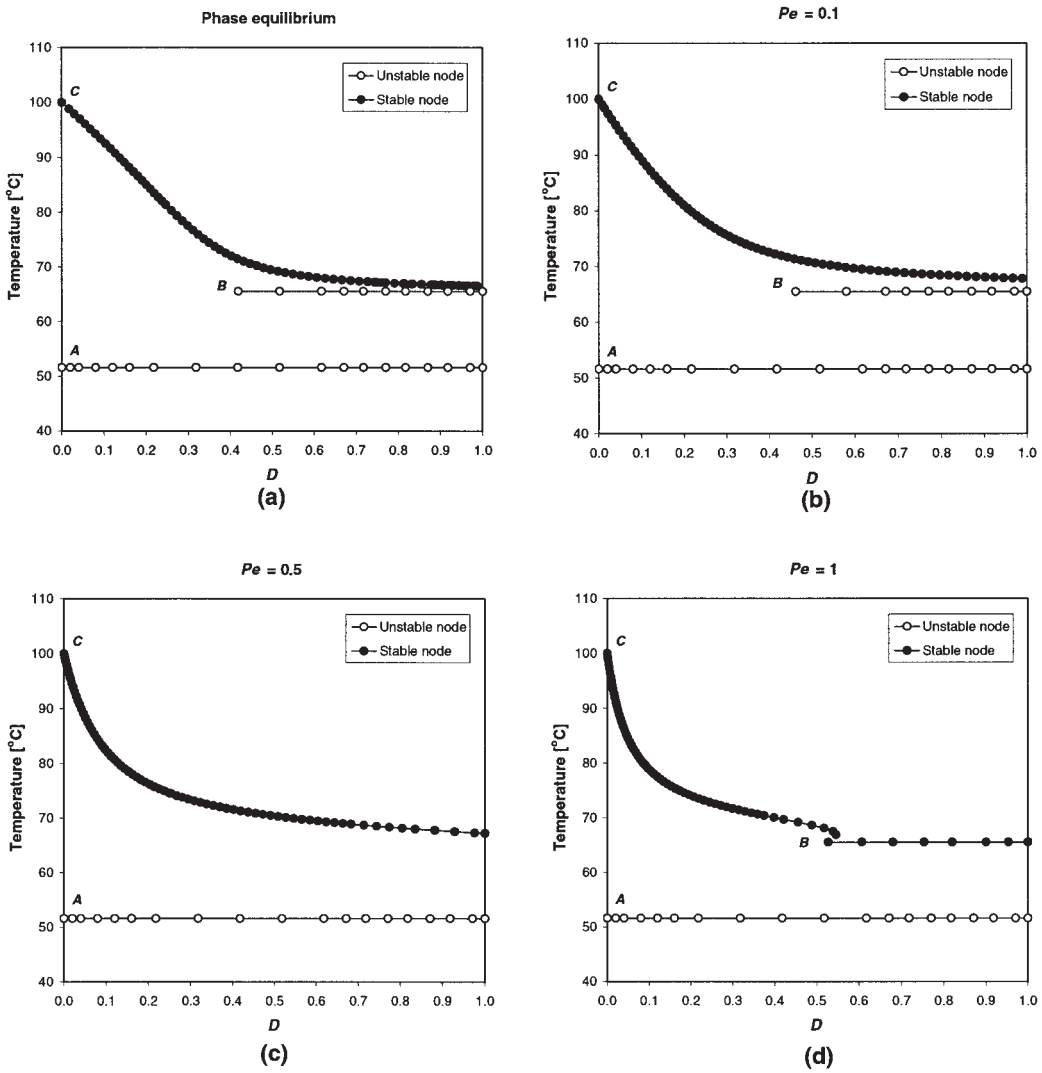

Figure 9. Feasibility diagram (different $\kappa_{i,k}$).

(a) Phase equilibrium case; (b) Pe = 0.1; (c) Pe = 0.5; (d) Pe = 1.

(Antoine vapor pressure equation and the NRTL equation for activity coefficients, including vapor-phase dimerization of acetic acid) were taken from Venimadhavan et al. (1999, Table 3). When we apply the fixed-point cascade model with $\phi = 0.5$ to this specific example the following equations for the stripping and rectifying cascades, respectively, are solved

$$(1 - D)(\hat{x}_i - \hat{y}_i) + 2D\left(\hat{x}_1\hat{x}_2 - \frac{\hat{x}_3\hat{x}_4}{8.7}\right)\nu_i = 0 \qquad i = 1, 2, 3 \tag{58}$$

$$(1 - D)(\hat{x}_i - \hat{y}_i) - 2D\left(\hat{x}_1\hat{x}_2 - \frac{\hat{x}_3\hat{x}_4}{8.7}\right)\nu_i = 0 \qquad i = 1, 2, 3 \tag{59}$$

Figure 11a is the bifurcation diagram of the stripping cascade fixed points obtained for the limit of no mass transfer resistance. The corresponding bifurcation diagram for the rectifying cascade fixed points is shown in Figure 11b. The unstable node branches of the rectifying cascade and the stable node branches of the stripping cascade are combined to give the feasibility diagram in Figure 12. For $D \leq 0.395$ acetic acid can be obtained as the bottom product from a continuous reactive distillation. For $D \geq 0.395$ either IPA or acetic acid are potential bottom products, depending on which distillation region contains the feed composition. The potential distillates (unstable nodes in the rectifying cascade and feasibility bifurcation diagrams) are quaternary mixtures of composition determined by the Da number.

We calculate the fixed points for the case of finite mass-transfer rates and compare them with those at phase equilibrium. We consider the general case of mass transfer in both the liquid phase and the vapor phase, and use film theory to estimate the binary mass-transfer coefficients from binary diffusivities ($\kappa_{i,k} = D_{i,k}/l$, where l is the film thickness). Vapor-phase mass transfer affects only the rectifying cascade trajectories, leaving the fixed-point limit unchanged (see Appendix).

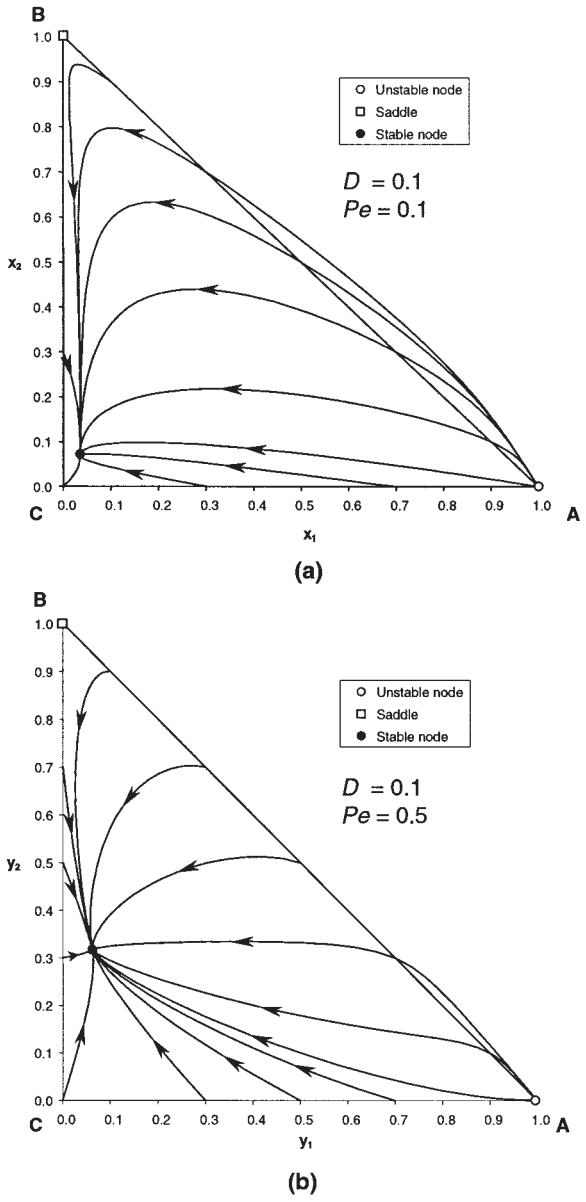

Figure 10. Phase planes for the ABC example at low *D*.

(a) Stripping cascade (equal $\kappa_{i,k}$); (b) rectifying cascade (different $\kappa_{i,k}$).

The vapor-phase binary diffusivities can be estimated using the Chapman–Enskog model (Reid et al., 1987, p. 581). The liquid-phase binary diffusivities ($D^L_{i,k}$) were estimated from the infinite-dilution binary diffusivities ($D^0_{i,k}$), which are calculated using the Wilke–Chang model (Reid et al., 1987, p. 598). The vapor and liquid binary diffusivities used in the calculations (Stefan–Maxwell binary diffusivities) are listed in Table 2.

To calculate the binary mass-transfer coefficients from the binary diffusivities we assumed a film thickness of 1 mm for the vapor phase, which is a typical value for other systems involving low molecular weight aliphatic alcohols and esters (for example, Taylor and Krishna, 1993, pp. 157, 170, 191, 201), and a film thickness of 0.1 mm for the liquid phase, a value already used for the ethyl acetate system (Kenig et al., 2000). When a priori estimates of the film thickness cannot be made, the mass-transfer coefficients are estimated using empirical correlations (Sherwood et al., 1975, Chapters 5 and 6; Taylor and Krishna, 1993, Chapter 8, section 8). The values of binary mass-transfer coefficients used in the simulations are listed in Table 2 and are used to calculate the multicomponent mass-transfer coefficients according to Eqs. 32 and 37. Those multicomponent mass transfer coefficients are the low-flux mass-transfer coefficients, which are assumed equal to the high-flux mass-transfer coefficients, given that the high flux correction factor (Taylor and Krishna, 1993, p. 143) was found to be negligible in distillation (Kooijman and Taylor, 1995a; Powers et al., 1988).

We choose $k^L_{ref} = \max(\kappa^L_{i,k}) = 8.28 \times 10^{-3}$ cm/s and $k^V_{ref} = \max(\kappa^V_{i,k}) = 1.74$ cm/s. The value of interfacial area per unit

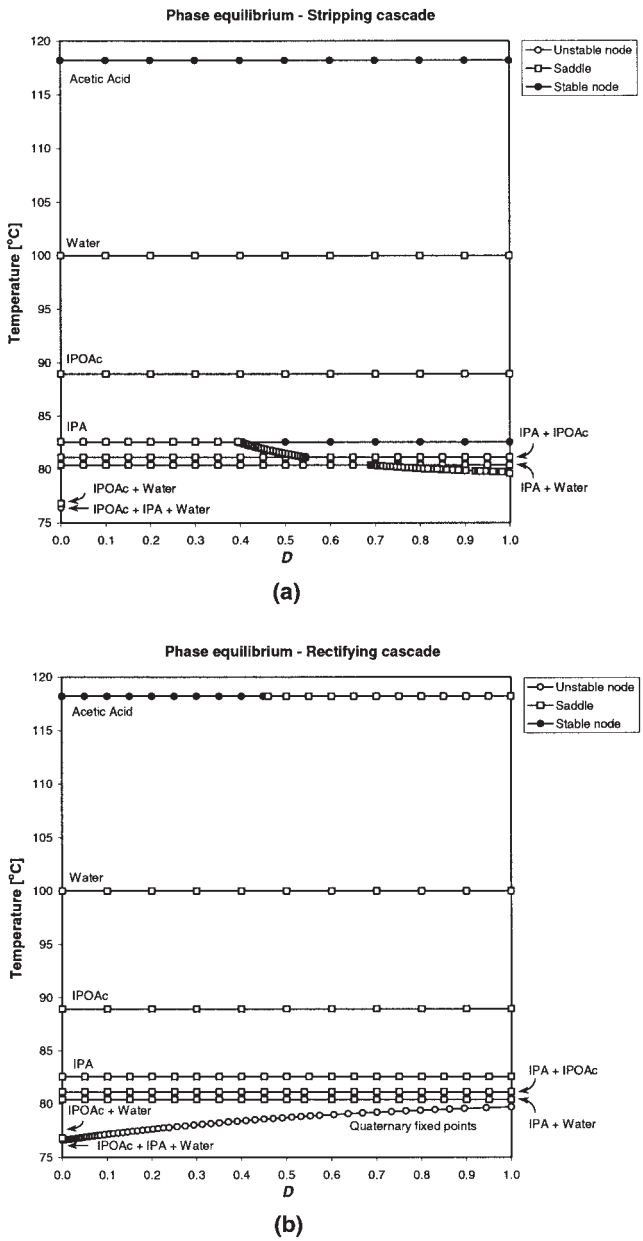

Figure 11. Isopropyl acetate example.

Stripping cascade (a) and rectifying cascade (b) bifurcation diagrams for the phase equilibrium case.

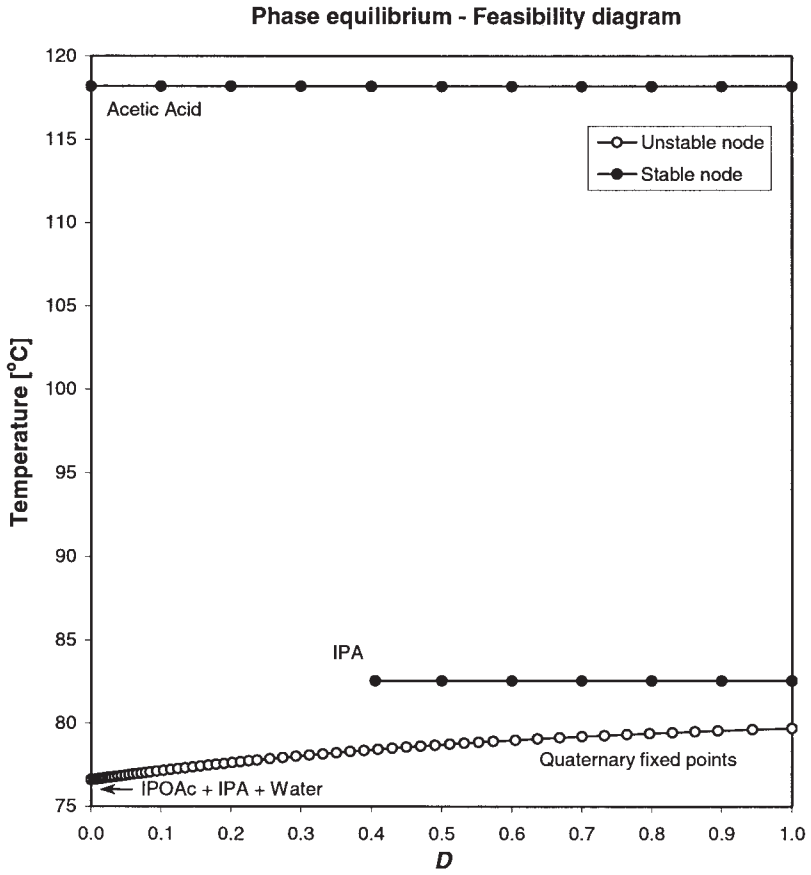

Figure 12. Isopropyl acetate example.

Feasibility diagram for the phase equilibrium case.

volume greatly depends on the equipment design and the fluid dynamic regime. For tray columns, values between approximately 450 and 2000 m^2/m^3 are reported, depending on the hydrodynamics on the tray (Taylor and Krishna, 1993, Chapter 12). We use an interfacial area of 1000 m^2/m^3 for both the liquid phase and the vapor phase. If we consider a liquid residence time of 2 min and a vapor residence time of 1 s we obtain $Pe^L = 1.01 \times 10^{-1}$ and $Pe^V = 5.75 \times 10^{-2}$. We now calculate the fixed points and their stability for increasing values of the Pe number, starting from the base case ($Pe^L = Pe_0^L = 0.101$ and $Pe^V = Pe_0^V = 0.0575$), until we detect a change in the feasibility diagram.

Table 2. Isopropyl Acetate Example: Binary Diffusivities and Mass Transfer Coefficients

Diffusivities (cm^2/s)	
Vapor Phase	Liquid Phase
$D_{1,2} = 7.29 \times 10^{-2}$	$D_{1,2} = 4.22 \times 10^{-5}$
$D_{1,3} = 5.61 \times 10^{-2}$	$D_{1,3} = 4.93 \times 10^{-5}$
$D_{1,4} = 1.74 \times 10^{-1}$	$D_{1,4} = 6.37 \times 10^{-5}$
$D_{2,3} = 5.26 \times 10^{-2}$	$D_{2,3} = 5.48 \times 10^{-5}$
$D_{2,4} = 1.65 \times 10^{-1}$	$D_{2,4} = 7.09 \times 10^{-5}$
$D_{3,4} = 1.36 \times 10^{-1}$	$D_{3,4} = 8.28 \times 10^{-5}$
Binary Mass Transfer Coefficients (cm/s)	
Vapor Phase	Liquid Phase
$\kappa_{1,2} = 0.729$	$\kappa_{1,2} = 4.22 \times 10^{-3}$
$\kappa_{1,3} = 0.561$	$\kappa_{1,3} = 4.93 \times 10^{-3}$
$\kappa_{1,4} = 1.74$	$\kappa_{1,4} = 6.37 \times 10^{-3}$
$\kappa_{2,3} = 0.526$	$\kappa_{2,3} = 5.48 \times 10^{-3}$
$\kappa_{2,4} = 1.65$	$\kappa_{2,4} = 7.09 \times 10^{-3}$
$\kappa_{3,4} = 1.36$	$\kappa_{3,4} = 8.28 \times 10^{-3}$

The fixed points calculated for the above values of Pe number are essentially the same as those at phase equilibrium. The topology of all the branches remains unchanged and the bifurcation points are close to the phase equilibrium case. Thus the mass-transfer resistances have a negligible effect on feasibility for this case.

As we increase the value of Pe we start to observe small changes in the position of the bifurcation points. To detect a significant change in the fixed point maps we need to increase Pe by a factor of 11 ($Pe_0^L = 1.11$ and $Pe_0^V = 0.633$). The fixed points calculated for those values of Pe are shown in Figure 13. In the stripping cascade (Figure 13a) the bifurcation point in the pure IPA branch is still present, although the branch remains a branch of saddles for all values of D (the IPA stable nodes disappear). The branch of saddles that connected the bifurcation point of the pure IPA branch with the bifurcation point of the IPA–IPOAc branch has a bifurcation point at $D = 0.64$: the fixed points corresponding to values of D between 0.64 and 0.68 are now stable nodes. For $D > 0.68$ the IPA–IPOAc is a branch of stable nodes. Because of the changes in the stable node branches of the stripping cascade the feasibility

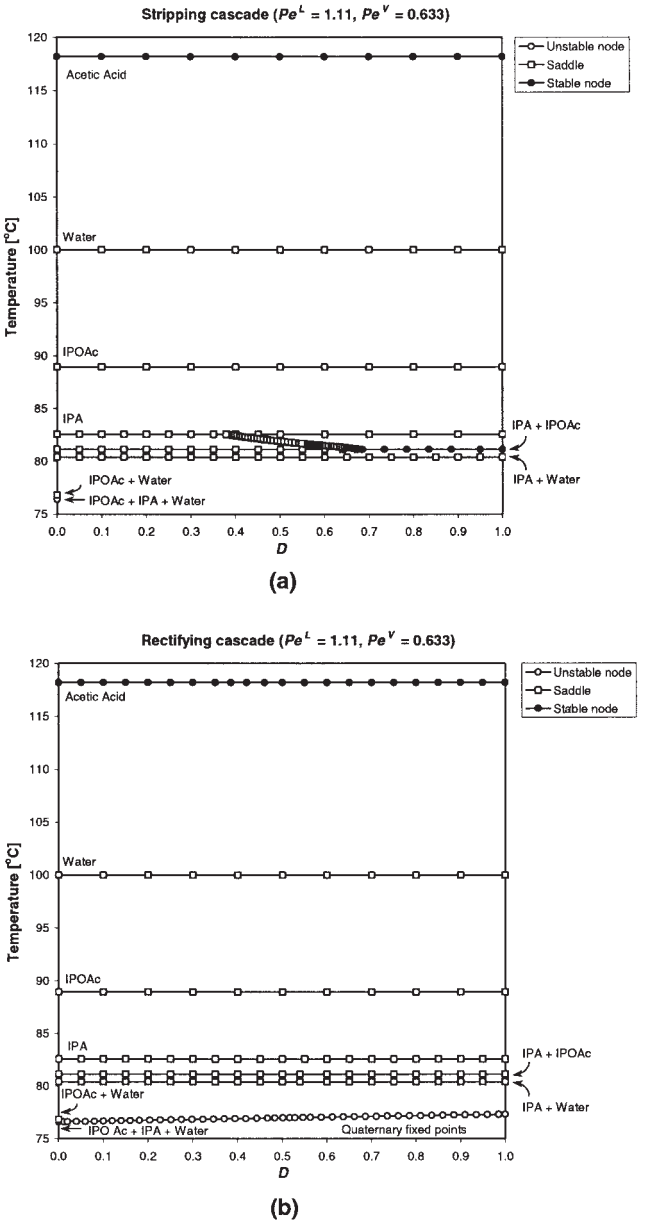

Figure 13. Isopropyl acetate example.

Stripping cascade (a) and rectifying cascade (b) bifurcation diagrams for $Pe^L = 1.11$ and $Pe^V = 0.633$.

diagram (Figure 14) is different: pure IPA is no longer a possible bottom product. Instead, the IPA–IPOAc azeotrope together with a short branch of quaternary fixed points are feasible bottom compositions of a continuous column, depending on the feed composition and the value of Da.

In conclusion, the IPOAc system can be well described using phase equilibrium for realistic values of the operating parameters (holdups and interfacial areas given by typical distillation conditions). For values of Pe corresponding to those operating conditions, the fixed points are almost indistinguishable from the equilibrium case. When mass-transfer resistances increase significantly (that is, by a factor of 11) the bifurcation and feasibility diagrams can change, leading to different feasible products in a continuous reactive distillation system. Physically we can think of changing mass-transfer resistance (changing Pe numbers) by changing the mass-transfer coefficients (such as different mixing regimes or gas–liquid velocities) or by changing interfacial area, which could be achieved, for instance, by changing the characteristic bubble size in the system. Changes by an order of magnitude in mass-transfer coefficient or interfacial area are not uncommon in certain types of equipment, depending on operating conditions (for example, Al-Dahhan et al., 1997; Sada et al., 1987; Sundaresan and Varma, 1990; Tekie et al., 1997; Veljkovic and Scala, 1988), although such changes are generally possible in laboratory-scale equipments that are designed to explore the largest possible intervals of operating conditions regardless of economic constraints, which are considered when designing a commercial unit operation.

Conclusions

The effect of mass-transfer resistance has been considered for feasibility of a reactive distillation process. Starting from the flash cascade framework, introduced by Chadda et al. (2001), we have accounted for the presence of mass-transfer resistances in both vapor and liquid phases using the Stefan–Maxwell equations. In addition to the two dimensionless groups previously defined to describe reactive distillation systems at phase equilibrium (Damköhler number Da and vapor fraction ϕ) a new dimensionless parameter (Peclet number Pe) is introduced for quantifying the effect of finite mass-transfer rates.

As in the case of phase equilibrium we focus our attention on the bifurcation analysis of the fixed-point equations (Chadda et al., 2001; Venimadhavan et al., 1999) because it provides a useful tool for determining feasible splits in a continuous reactive distillation column. The results are shown in bifurcation diagrams and feasibility diagrams that are constructed as a function of the dimensionless Damköhler number D for different values of the Pe number. For low values of Pe the limit of phase equilibrium is recovered. As mass-transfer resistances increase (higher Pe) the position (relative to D) and the topology of the fixed points may change, leading to differences in the composition trajectories and ultimately in the feasible splits achievable in a certain kinetic regime (specified by D).

The fixed-point analysis was performed for two reactive distillation examples. First we report a parametric study on the idealized reaction $A + B \rightleftharpoons C$, then we analyze the esterification of acetic acid and isopropanol to make isopropyl acetate. For both examples in the limit of no reaction ($D \to 0$) mass transfer does not affect feasibility because the fixed points do not change regardless of the magnitude of the mass-transfer resistance. For the isopropyl acetate system we showed that for typical values of mass-transfer coefficients the approximation of phase equilibrium is perfectly acceptable. To significantly change the feasibility diagram (and therefore the type of feasible splits) an increase of about one order of magnitude in mass-transfer resistance is necessary. Such a change in mass-transfer rate might not always be possible to realize in a particular system, depending on the type of equipment and operating conditions. Nevertheless the important point we want to convey is that in the conceptual design phase a feasibility study, including mass transfer, might show the possibility of obtaining compositions that could otherwise be overlooked if only the phase equilibrium model is considered. Then the likelihood of being able to practically attain those compositions

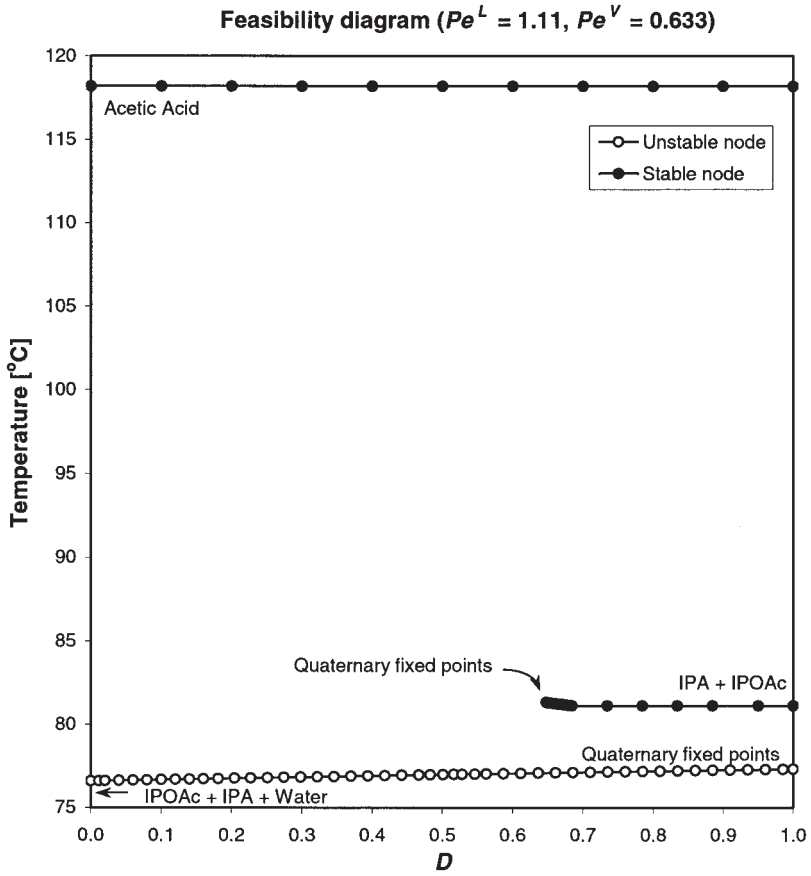

Figure 14. Isopropyl acetate example.

Feasibility diagram for $Pe^L = 1.11$ and $Pe^V = 0.633$.

by reducing or increasing mass-transfer rates will depend on the magnitude of the required mass-transfer resistance and the availability of commercial equipment to induce it.

Acknowledgments

We are grateful to Prof. Ross Taylor for his helpful advice.

Notation

a = interfacial area per unit volume, 1/m
A = interfacial area, m^2
a_i = activity of component i
C = total number of components
D = scaled Damköhler number
$D_{i,k}$ = binary diffusivity, cm^2/s
Da = first Damköhler number
H_j = holdup in unit j, mol
K_{eq} = reaction equilibrium constant
k_f = forward reaction rate constant, 1/s
$k_{f,ref}$ = forward reaction rate constant at the reference temperature, 1/s
$k_{i,k}$ = multicomponent mass-transfer coefficient, m/s
k_{ref} = reference mass-transfer coefficient, m/s
l = film thickness, m
L = liquid flow rate, kmol/s
$M(\mathbf{x})$ = average molecular weight ($= \sum_{i=1}^{C} M_i x_i$) (also valid for $\mathbf{y}$ instead of $\mathbf{x}$)
M = index for rectifying cascade flash unit
N = index for stripping cascade flash unit
N_i = mass-transfer rate of component i, kmol/s
N_T = total mass-transfer rate, kmol/s
P = system pressure, Pa
Pe = Peclet number
$r(\mathbf{x})$ = driving force for the reaction, moles reacted per mole of mixture
T = temperature, °C
V = vapor flow rate, kmol/s
$\mathbf{x}$ = state vector
x_i = mole fraction of component i in the liquid phase
x_i^I = interfacial mole fraction of component i in the liquid phase
$\bar{x}_i$ = average (between bulk and interface) mole fraction of component i in the liquid phase
y_i = mole fraction of component i in the vapor phase
y_i^I = interfacial mole fraction of component i in the liquid phase

Greek letters

γ_i = liquid activity coefficient of component i
$\Gamma_{i,k}$ = thermodynamic factor
$\kappa_{i,k}$ = binary mass-transfer coefficient, m/s
ν_i = stoichiometric coefficient of component i
ν_T = summation of all stoichiometric coefficients
ρ = molar density, $kmol/m^3$
ϕ_j = fraction of feed vaporized in jth flash unit

Subscripts and Superscripts

0 = initial condition
F = feed
i = component index
I = interface
j = stage index for flash cascade
k = component index
L = liquid phase
m = mass-based quantity

ref = reference
V = vapor phase
$\wedge$ = pinch composition

Literature Cited

Agarwal, S., and R. Taylor, "Distillation Column Design Calculations Using a Nonequilibrium Model," *Ind. Eng. Chem. Res.*, **33**, 2631 (1994).

Agreda, V. H., and L. R. Partin, "Reactive Distillation Process for the Production of Methyl Acetate," U.S. Patent No. 4,435,595 (1984).

Agreda, V. H., L. R. Partin, and W. H. Heise, "High Purity Methyl Acetate via Reactive Distillation," *Chem. Eng. Prog.*, **86**(2), 40 (1990).

Al-Dahhan, M. H., F. Larachi, M. P. Dudukovic, and A. Laurent, "High-Pressure Trickle- Bed Reactors: A Review," *Ind. Eng. Chem. Res.*, **36**, 3292 (1997).

Barbosa, D., and M. F. Doherty, "The Simple Distillation of Homogeneous Reactive Mixtures," *Chem. Eng. Sci.*, **43**, 541 (1988).

Castillo, F. J. L., and G. P. Towler, "Azeotropic Distillation Design Considering Mass Transfer Rates," *IChemE Symp. Ser.*, **142**, 625 (1997).

Castillo, F. J. L., and G. P. Towler, "Influence of Multicomponent Mass Transfer on Homogeneous Azeotropic Distillation," *Chem. Eng. Sci.*, **53**, 963 (1998).

Chadda, N., M. F. Malone, and M. F. Doherty, "Feasible Products for Kinetically Controlled Reactive Distillation of Ternary Mixtures," *AIChE J.*, **46**, 923 (2000).

Chadda, N., M. F. Malone, and M. F. Doherty, "Effect of Chemical Kinetics on Feasible Splits for Reactive Distillation," *AIChE J.*, **47**, 590 (2001).

Chiplunkar, M., M. F. Doherty, M. F. Malone, and M. Hong, "Experimental Study of Feasibility in Kinetically-Controlled Reactive Distillation," *AIChE Annual Meeting*, Paper No. 368c (2001).

Ciric, A. R., and D. Gu, "Synthesis of Nonreactive Reactive Distillation Processes by MINLP Optimization," *AIChE J.*, **40**, 1479 (1994).

Damköhler, G., "Strömungs und Wärme übergangsprobleme in Chemischer Technik und Forschung," *Chem. Eng. Technol.*, **12**, 469 (1939).

Doedel, E., "AUTO: Software for Continuation and Bifurcation Problems in Ordinary Differential Equations," Dept. of Mathematics, California Institute of Technology, Pasadena, CA (1986).

Doherty, M. F., and M. F. Malone, *Conceptual Design of Distillation Systems*, McGraw-Hill, New York (2001).

Espinosa, J., P. A. Aguirre, and G. A. Perez, "Product Composition Regions of Single-Feed Reactive Distillation Columns: Mixtures Containing Inerts," *Ind. Eng. Chem. Res.*, **34**, 853 (1995).

Fidkowski, Z. T., M. F. Doherty, and M. F. Malone, "Feasibility of Separations for Distillation of Nonideal Ternary Mixtures," *AIChE J.*, **39**, 1303 (1993).

Froment, G. F., and K. B. Bischoff, *Chemical Reactor Analysis and Design*, 2nd Edition, Wiley, New York (1990).

Gadewar, S. B., M. F. Malone, and M. F. Doherty, "Feasible Region for a Countercurrent Cascade of Vapor–Liquid CSTRs," *AIChE J.*, **48**, 800 (2002).

Henley, E. J., and J. D. Seader, *Equilibrium-Stage Separation Operations in Chemical Engineering*, Wiley, New York (1981).

Higler, A., R. Krishna, and R. Taylor, "Nonequilibrium Cell Model for Multicomponent (Reactive) Separation Processes," *AIChE J.*, **45**, 2357 (1999a).

Higler, A., R. Taylor, and R. Krishna, "Modeling of a Reactive Separation Process Using a Nonequilibrium Stage Model," *Comp. Chem. Eng.*, **22**, S111 (1998).

Higler, A., R. Taylor, and R. Krishna, "The Influence of Mass Transfer and Mixing on the Performance of a Tray Column for Reactive Distillation," *Chem. Eng. Sci.*, **54**, 2873 (1999b).

Higler, A., R. Taylor, and R. Krishna, "Nonequilibrium Modeling of Reactive Distillation: A Dusty Fluid Model for Heterogeneously Catalyzed Processes," *Ind. Eng. Chem. Res.*, **39**, 1596 (2000).

Ismail, S. R., E. N. Pistikopoulos, and K. P. Papalexandri, "Synthesis of Reactive and Combined Reactor/Separation Systems Utilizing a Mass/Heat Exchange Transfer Module," *Chem. Eng. Sci.*, **54**, 2721 (1999).

Kenig, E. Y., F. Butzmann, L. Kucka, and A. Gorak, "Comparison of Numerical and Analytical Solutions of a Multicomponent Reaction-Mass-Transfer Problem in Terms of the Film Model," *Chem. Eng. Sci.*, **55**, 1483 (2000).

Kooijman, H. A., and R. Taylor, "Modeling Mass Transfer in Multicomponent Distillation," *Chem. Eng. J.*, **57**, 177 (1995a).

Kooijman, H. A., and R. Taylor, "A Nonequilibrium Model for Dynamic Simulation of Tray Distillation Columns," *AIChE J.*, **41**, 1852 (1995b).

Lee, J. W., S. Hauan, and A. W. Westerberg, "Circumventing an Azeotrope in Reactive Distillation," *Ind. Eng. Chem. Res.*, **39**, 1061 (2000a).

Lee, J. W., S. Hauan, and A. W. Westerberg, "Graphical Methods for Reactive Distribution in a Reactive Distillation Column," *AIChE J.*, **46**, 1218 (2000b).

Lee, L.-S., and M.-Z. Kuo, "Phase and Reaction Equilibria of the Isopropanol–Acetic Acid–Isopropyl Acetate–Water System at 760 mm Hg," *Fluid Phase Equilib.*, **123**, 147 (1996).

Malone, M. F., and M. F. Doherty, "Reactive Distillation," *Ind. Eng. Chem. Res.*, **39/40**, 3953 (2000).

Manning, J., "Kinetics and Feasibility of Reactive Distillation in Isopropyl Acetate Synthesis," MS Thesis, University of Massachusetts, Amherst, MA (2000).

McGregor, C., D. Glasser, and D. Hildebrandt, "Process Synthesis of a Reactive Distillation System Using Attainable Region Results," *Distillation and Absorption '97, IChemE Symp. Ser.*, **142**, 663 (1997).

Nisoli, A., M. F. Malone, and M. F. Doherty, "Attainable Regions for Reaction with Separation," *AIChE J.*, **43**, 374 (1997).

Oyevaar, M. H., B. W. To, M. F. Doherty, and M. F. Malone, "Process for Continuous Production of Carbonate Esters," U.S. Patent No. 6,093,842 (2000).

Papalexandri, K. P., and E. N. Pistikopoulos, "Generalized Modular Representation for Process Synthesis," *AIChE J.*, **42**, 1010 (1996).

Powers, M. F., D. J. Vickery, A. Arehole, and R. Taylor, "A Nonequilibrium Stage Model of Multicomponent Separation Processes—V. Computational Methods for Solving the Model Equations," *Comput. Chem. Eng.*, **12**, 1229 (1988).

Reid, R. C., J. M. Prausnitz, and B. E. Poling, *The Properties of Gases and Liquids*, 4th Edition, McGraw-Hill, New York (1987).

Rev, E., "Reactive Distillation and Kinetic Azeotropy," *Ind. Eng. Chem. Res.*, **33**, 2174 (1994).

Sada, E., H. Kumazawa, C. H. Lee, and H. Narukawa, "Gas–Liquid Interfacial Area and Liquid-Side Mass-Transfer Coefficient in a Slurry Bubble Column," *Ind. Eng. Chem. Res.*, **26**, 112 (1987).

Sherwood, T. K., R. L. Pigford, and C. R. Wilke, *Mass Transfer*, McGraw-Hill, New York (1975).

Sridhar, L. N., C. Maldonado, and A. M. Garcia, "Design and Analysis of Nonequilibrium Separation Processes," *AIChE J.*, **48**, 1179 (2002).

Sundaresan, A., and Y. B. G. Varma, "Interfacial Area and Mass Transfer in Gas–Liquid Cocurrent Upflow and Countercurrent Flow in Reciprocating Plate Column," *Can. J. Chem. Eng.*, **68**, 952 (1990).

Sundmacher, K., and U., Hoffmann, "Activity Evolution of a Catalytic Distillation Packing for MTBE Production," *Chem. Eng. Technol.*, **16**, 279 (1993).

Sundmacher, K., and U., Hoffmann, "Multicomponent Mass and Energy Transport on Different Length Scales in a Packed Reactive Distillation Column for Heterogeneously Catalyzed Fuel Ether Production," *Chem. Eng. Sci.*, **49**, 4443 (1994).

Sundmacher, K., L. K. Rihko, and U. Hoffmann, "Classification of Reactive Distillation Processes by Dimensionless Numbers," *Chem. Eng. Commun.*, **127**, 151 (1994).

Taylor, R., and H. A. Kooijman, "Composition Derivatives of Activity Coefficient Models (for the Estimation of Thermodynamic Factors in Diffusion)," *Chem. Eng. Commun.*, **102**, 87 (1991).

Taylor, R., and R. Krishna, *Multicomponent Mass Transfer*, Wiley, New York (1993).

Taylor, R., and R. Krishna, "Modelling Reactive Distillation," *Chem. Eng. Sci.*, **55**, 5183 (2000).

Tekie, Z., J. Li, and B. I. Morsi, "Mass Transfer Parameters of O_2 and N_2 in Cyclohexane under Elevated Pressures and Temperatures: A Statistical Approach," *Ind. Eng. Chem. Res.*, **36**, 3879 (1997).

Thiel, C., K. Sundmacher, and U. Hoffmann, "Residue Curve Maps for Heterogeneously Catalysed Reactive Distillation of Fuel Ethers MTBE and TAME," *Chem. Eng. Sci.*, **52**, 993 (1997a).

Thiel, C., K. Sundmacher, and U. Hoffmann, "Synthesis of ETBE: Residue Curve Maps for the Heterogeneously Catalyzed Reactive Distillation Processes," *Chem. Eng. J.*, **66**, 181 (1997b).

Ung, S., and M. F. Doherty, "Necessary and Sufficient Conditions for Reactive Azeotropes in Multireaction Mixtures," *AIChE J.*, **41**, 2383 (1995a).

Ung, S., and M. F. Doherty, "Synthesis of Reactive Distillation Systems with Multiple Equilibrium Chemical Reactions," *Ind. Eng. Chem. Res.*, **34**, 2555 (1995b).

Ung, S., and M. F. Doherty, "Calculation of Residue Curve Maps for Mixtures with Multiple Equilibrium Chemical Reactions," *Ind. Eng. Chem. Res.*, **34**, 3195 (1995c).
Vas Bath, R. D., W. P. M. van Swaaij, J. A. M. Kuipers, and G. F. Versteeg, "Mass Transfer with Complex Chemical Reaction in Gas-Liquid Systems—I. Consecutive Reversible Reactions with Equal Diffusivities," *Chem. Eng. Sci.*, **54**, 121 (1999a).
Vas Bath, R. D., W. P. M. van Swaaij, J. A. M. Kuipers, and G. F. Versteeg, "Mass Transfer with Complex Chemical Reaction in Gas–Liquid Systems—II: Effect of Unequal Diffusivities on Consecutive Reactions," *Chem. Eng. Sci.*, **54**, 137 (1999b).
Veljkovic, V., and D. Skala, "Mass Transfer Characteristics in a Gas–Liquid Reciprocating Plate Column—II. Interfacial Area," *Can. J. Chem. Eng.*, **66**, 200 (1988).
Venimadhavan, G., M. F. Malone, and M. F. Doherty, "Effect of Kinetics on Residue Curve Maps for Reactive Distillation," *AIChE J.*, **40**, 1814 (1994) [Correction: *AIChE J.*, **41**, 2613 (1995)].
Venimadhavan, G., M. F. Malone, and M. F. Doherty, "Bifurcation Study of Kinetic Effects in Reactive Distillation," *AIChE J.*, **45**, 546 (1999).
Wahnschafft, O. M., J. W. Koehler, E. Blass, and A. W. Westerberg, "The Product Composition Regions of Single-Feed Azeotropic Distillation Columns," *Ind. Eng. Chem. Res.*, **31**, 2345 (1992).

Appendix: Independence of Fixed-Point Equations from Vapor-Phase Mass Transfer

In the derivation of the mass-transfer model we mentioned that the fixed-point equations are independent of the vapor-phase mass-transfer resistances. A simple way to show this is to couple the vapor-phase mass balances (Eq. 10) with the vapor-phase mass-transfer rate equations (Eq. 14), to eliminate the vapor phase mass-transfer rates $N^V_{i,j}$.

Stripping cascade

The vapor-phase component mass balance (Eq. 10) and overall mass balance are equivalent to

$$N^V_{i,j} = V_j y_{i,j} \qquad i = 1, \ldots, C-1 \tag{A1}$$

$$N^V_{T,j} = V_j \tag{A2}$$

If we substitute Eqs. A1 and A2 into the mass-transfer rate Eq. 14 we obtain

$$V_j y_{i,j} - \rho^V_j \sum_{k=1}^{C-1} k^V_{i,k,j}(y^I_{k,j} - y_{k,j}) A_j - y_{i,j} V_j = 0 \qquad i = 1, \ldots, C-1 \tag{A3}$$

which simplifies to

$$\rho^V_j \sum_{k=1}^{C-1} k^V_{i,k,j}(y^I_{k,j} - y_{k,j}) A_j = 0 \qquad i = 1, \ldots, C-1 \tag{A4}$$

or, in dimensionless form

$$\frac{1}{\mathrm{Pe}^V} \sum_{k=1}^{C-1} \frac{k^V_{i,k,j}}{k^V_{ref}} (y^I_{k,j} - y_{k,j}) = 0 \qquad i = 1, \ldots, C-1 \tag{A5}$$

The corresponding fixed-point equation is

$$\frac{1}{\mathrm{Pe}^V} \sum_{k=1}^{C-1} \frac{k^V_{i,k}}{k^V_{ref}} (\hat{y}^I_k - \hat{y}_k) = 0 \qquad i = 1, \ldots, C-1 \tag{A6}$$

The solution of both Eqs. A5 and A6 is $y^I_i = y_i$, independent of the mass-transfer resistances in the vapor phase expressed by the dimensionless number Pe^V, which cancels out in the equations. An analogous situation is encountered in multicomponent condensation (Taylor and Krishna, 1993, Chapter 15), when it is assumed that the condensate is completely mixed ($x^I_i = x_i$).

Rectifying cascade

The vapor-phase component mass balance and overall mass balance are equivalent to

$$N^V_{i,j} = V_j y_{i,j} - V_{j-1} y_{i,j-1} \qquad i = 1, \ldots, C-1 \tag{A7}$$

$$N^V_{T,j} = V_j - V_{j-1} \tag{A8}$$

If we substitute Eqs. A7 and A8 into the mass-transfer rate Eq. 14 we obtain

$$V_j y_{i,j} - V_{j-1} y_{i,j-1} - \rho^V_j \sum_{k=1}^{C-1} k^V_{i,k,j}(y^I_{k,j} - y_{k,j}) A_j - y_{i,j}(V_j - V_{j-1}) = 0 \qquad i = 1, \ldots, C-1 \tag{A9}$$

which simplifies to

$$\rho^V_j \sum_{k=1}^{C-1} k^V_{i,k,j}(y^I_{k,j} - y_{k,j}) A_j + V_{j-1}(y_{i,j-1} - y_{i,j}) = 0 \qquad i = 1, \ldots, C-1 \tag{A10}$$

or, in dimensionless form

$$\frac{1}{\mathrm{Pe}^V} \sum_{k=1}^{C-1} \frac{k^V_{i,k,j}}{k^V_{ref}} (y^I_{k,j} - y_{k,j}) + (y_{i,j-1} - y_{i,j}) = 0 \qquad i = 1, \ldots, C-1 \tag{A11}$$

The corresponding fixed-point equation is

$$\frac{1}{\mathrm{Pe}^V} \sum_{k=1}^{C-1} \frac{k^V_{i,k}}{k^V_{ref}} (\hat{y}^I_k - \hat{y}_k) = 0 \qquad i = 1, \ldots, C-1 \tag{A12}$$

Although the solution of Eq. A11 depends on Pe^V (as in multicomponent condensation), the solution of the corresponding fixed-point Eq. A12 is independent of the mass-transfer resistances in the vapor phase. Therefore, for the rectifying section, the cascade trajectories change as the mass-transfer resistance changes, but the fixed points will be the same regardless of the value of Pe^V.

Manuscript received Feb. 15, 2003, and revision received Sep. 25, 2003.